

# **Supplementary Data**

## **Mitochondrial DNA deletions are associated with non-B DNA conformations**

Joana Damas<sup>1</sup>, João Carneiro<sup>1,2</sup>, Joana Gonçalves<sup>1</sup>, James B Stewart<sup>3</sup>, David C Samuels<sup>4</sup>, António Amorim<sup>1,2</sup>, Filipe Pereira<sup>1</sup>

<sup>1</sup> Institute of Molecular Pathology and Immunology of the University of Porto (IPATIMUP), Rua Dr. Roberto Frias s/n, 4200-465 Porto, Portugal

<sup>2</sup> Faculty of Sciences, University of Porto, Rua do Campo Alegre, s/n, 4169-007 Porto, Portugal

<sup>3</sup> Max Planck Institute for Biology of Ageing, Cologne, Germany

<sup>4</sup> Center for Human Genetic Research, Vanderbilt University Medical Center, Nashville, Tennessee, United States of America

## Contents

Supplemental Figure S1. List of published studies from which deletions were retrieved.	3
Supplemental Figure S2. Refinement of breakpoint locations on the revised Cambridge reference mtDNA sequence (rCRS).	6
Supplemental Figure S3. List of the 753 unique mtDNA deletions used in this study.	7
Supplemental Figure S4. Distribution of 5' deletion breakpoints in the human mtDNA.	11
Supplemental Figure S5. Distribution of 3' deletion breakpoints in the human mtDNA.	12
Supplemental Figure S6. Distribution of 3' breakpoints around the 16,071 hotspot.	13
Supplemental Figure S7. List of the most frequent breakpoints detected in real and simulated mtDNA deletions.	14
Supplemental Figure S8. Secondary structures around the most frequent 5' and 3' breakpoint sites of the human mtDNA L-strand.	15
Supplemental Figure S9. Secondary structures around the most frequent 5' and 3' breakpoint sites of the human mtDNA H-strand.	17
Supplemental Figure S10. Global distribution of 5' breakpoints from deletions with the 3' breakpoint at the 16,071 hotspot.	20
Supplemental Figure S11. The WANCY cluster of tRNAs is a hotspot for mtDNA breakage.	21
Supplemental Figure S12. Distribution of deletion breakpoints according to the coding features of the mitochondrial genome.	22
Supplemental Figure S13. Number of mtDNA deletion breakpoints per base.	23
Supplemental Figure S14. Secondary structures of mitochondrial tRNA genes (L-strand).	24
Supplemental Figure S15. Secondary structures of mitochondrial tRNA genes (H-strand).	25
Supplemental Figure S16. Relationship between the folding free energy and the number of breakpoints in tRNA genes.	26
Supplemental Figure S17. The distribution of folding energies predicted for all of the 100-nt windows of the mitochondrial genome.	27
Supplemental Figure S18. Deletion hotspots and the mtDNA regions with high folding potentials.	28
Supplemental Figure S19. Descriptive statistics of folding energies in deletion breakpoints areas.	29
Supplemental Figure S20. Landscape of the folding potentials in the 5' breakpoint areas of mtDNA deletions.	30
Supplemental Figure S21. Landscape of the folding potentials in the 3' breakpoint area of mtDNA deletions.	33
Supplemental Figure S22. Comparison between the two main breakpoint hotspots and their flanking regions.	36

## Supplemental Figure S1. List of published studies from which deletions were retrieved.

- Almeida, E., H. Loureiro, et al. (2007). "Síndrome de Pearson. Caso clínico." *Acta Pediátrica Portuguesa* 38(2): 79-81.
- Andreu, A. L., M. G. Hanna, et al. (1999). "Exercise Intolerance Due to Mutations in the Cytochrome b Gene of Mitochondrial DNA." *New England Journal of Medicine* 341(14): 1037-1044.
- Bai, R.-K. and L.-J. C. Wong (2005). "Simultaneous Detection and Quantification of Mitochondrial DNA Deletion(s), Depletion, and Over-Replication in Patients with Mitochondrial Disease." *The Journal of Molecular Diagnostics* 7(5): 613-622.
- Bank, C., T. Soulimane, et al. (2000). "Multiple Deletions of mtDNA Remove the Light Strand Origin of Replication." *Biochemical and Biophysical Research Communications* 279(2): 595-601.
- Baumer, A., C. Zhang, et al. (1994). "Age-related Human mtDNA Deletions: A Heterogeneous Set of Deletions Arising at a Single Pair of Directly Repeated Sequences." *Am. J. Hum. Genet.* 54: 618-630.
- Behar, D. M., J. Blue-Smith, et al. (2008). "A novel 154-bp deletion in the human mitochondrial DNA control region in healthy individuals." *Human Mutation* 29(12): 1387-1391.
- Bender, A., K. J. Krishnan, et al. (2006). "High levels of mitochondrial DNA deletions in substantia nigra neurons in aging and Parkinson disease." *Nat Genet* 38(5): 515-517.
- Bi, R., A. M. Zhang, et al. (2010). "The acquisition of an inheritable 50-bp deletion in the human mtDNA control region does not affect the mtDNA copy number in peripheral blood cells." *Human Mutation* 31(5): 538-543.
- Blok, R. B., D. R. Thorburn, et al. (1995). "mtDNA Deletion in a Patient with Symptoms of Mitochondrial Cytopathy but without Ragged Red Fibers." *Biochemical and Molecular Medicine* 56(1): 26-30.
- Blok, R. B., D. R. Thorburn, et al. (1995). "A topoisomerase II cleavage site is associated with a novel mitochondrial DNA deletion." *Human Genetics* 95: 75-81.
- Bodyak, N. D., E. Nekhaeva, et al. (2001). "Quantification and sequencing of somatic deleted mtDNA in single cells: evidence for partially duplicated mtDNA in aged human tissues." *Human Molecular Genetics* 10(1): 17-24.
- Brierley, E. J., M. A. Johnson, et al. (1998). "Role of Mitochondrial DNA Mutations in Human Aging: Implications for the Central Nervous System and Muscle." *Annals of Neurology* 43(2): 217-223.
- Bua, E., J. Johnson, et al. (2006). "Mitochondrial DNA-Deletion Mutations Accumulate Intracellularly to Detrimental Levels in Aged Human Skeletal Muscle Fibers." *The American Journal of Human Genetics* 79(3): 469-480.
- Chabi, B., B. Mousson de Camaret, et al. (2003). "Quantification of Mitochondrial DNA Deletion, Depletion, and Overreplication: Application to Diagnosis." *Clin Chem* 49(8): 1309-1317.
- Corral-Debrinski, M., T. Horton, et al. (1992). "Mitochondrial DNA deletions in human brain: regional variability and increase with advanced age." *Nat Genet* 2: 324 - 329.
- Coulter-Mackie, M. B., D. A. Applegarth, et al. (1998). "A protocol for detection of mitochondrial DNA deletions: characterization of a novel deletion." *Clinical Biochemistry* 31(8): 627-632.
- Degoul, F., I. Nelson, et al. (1991). "Different mechanisms inferred from sequences of human mitochondrial DNA deletions in ocular myopathies." *Nucleic Acids Research* 19(3): 493-496.
- Eshaghian, A., R. A. Vleugels, et al. (2005). "Mitochondrial DNA Deletions Serve as Biomarkers of Aging in the Skin, but Are Typically Absent in Nonmelanoma Skin Cancers." *J Invest Dermatol* 126(2): 336-344.
- Fahn, H.-J., L.-S. Wang, et al. (1998). "Smoking-Associated Mitochondrial DNA Mutations and Lipid Peroxidation in Human Lung Tissues." *Am. J. Respir. Cell Mol. Biol.* 19(6): 901-909.
- Farlin, T., G. Guironnet, et al. (1997). "Detection of mitochondrial DNA deletions by a screening procedure using the Polymerase Chain Reaction." *Molecular and Cellular Biochemistry* 174(1): 221-225.
- Fischel-Ghodsian, N., M. C. Bohlman, et al. (1992). "Deletion in Blood Mitochondrial DNA in Kearns-Sayre Syndrome." *Pediatric Research* 31(6): 557-560.
- Fukushima, K. and C. Fiocchi (2004). "Paradoxical decrease of mitochondrial DNA deletions in epithelial cells of active ulcerative colitis patients." *American Journal of Physiology - Gastrointestinal and Liver Physiology* 286(5): G804-G813.
- Goios, A., C. Nogueira, et al. (2005). "mtDNA single macrodeletions associated with myopathies: Absence of haplogroup-related increased risk." *Journal of Inherited Metabolic Disease* 28(5): 769-778.
- Harbottle, A., K. J. Krishnan, et al. (2004). "Implications of Using the ND1 Gene as a Control Region for Real-Time PCR Analysis of Mitochondrial DNA Deletions in Human Skin." *J Investig Dermatol* 122(6): 1518-1521.
- Hayashi, J., S. Ohta, et al. (1991). "Introduction of disease-related mitochondrial DNA deletions into HeLa cells lacking mitochondrial DNA results in mitochondrial dysfunction." *Proceedings of the National Academy of Sciences* 88(23): 10614-10618.
- Holt, I. J., A. E. Harding, et al. (1989). "Deletions of muscle mitochondrial DNA in mitochondrial myopathies: sequence analysis and possible mechanisms." *Nucleic Acids Research* 17(12): 4465-4469.
- Horton, T. M., J. A. Petros, et al. (1996). "Novel Mitochondrial DNA Deletion Found in a Renal Cell Carcinoma." *Genes, Chromosomes & Cancer* 15: 95-101.
- Hsieh, R.-H., N.-M. Tsai, et al. (2002). "Multiple rearrangements of mitochondrial DNA in unfertilized human oocytes." *Fertility and Sterility* 77(5): 1012-1017.
- Jansson, M., N. Darin, et al. (2000). "Multiple mitochondrial DNA deletions in hereditary inclusion body myopathy." *Acta Neuropathologica* 100(1): 23-28.
- Kajander, O. A., A. T. Rovio, et al. (2000). "Human mtDNA sublimons resemble rearranged mitochondrial genomes found in pathological states." *Human Molecular Genetics* 9(19): 2821-2835.
- Kao, S. H., H. T. Chao, et al. (1998). "Multiple deletions of mitochondrial DNA are associated with the decline of motility and fertility of human spermatozoa." *Molecular Human Reproduction* 4(7): 657-666.
- Kapsa, R., G. N. Thompson, et al. (1994). "A Novel mtDNA Deletion in a Infant with Pearson Syndrome." *J. Inher. Metab. Dis.* 17: 521-526.
- Khrapko, K., N. Bodyak, et al. (1999). "Cell-by-cell scanning of whole mitochondrial genomes in aged human heart reveals a significant fraction of myocytes with clonally expanded deletions." *Nucleic Acids Research* 27(11): 2434-2441.

- Kleinle, S., U. Wiesmann, et al. (1997). "Detection and characterization of mitochondrial DNA rearrangements in Pearson and Kearns-Sayre syndromes by long PCR." *Human Genetics* 100(5): 643-650.
- Klopstock, T., F. Bischof, et al. (1995). "3.1-kb deletion of mitochondrial DNA in a patient with Kearns-Sayre syndrome." *Acta Neuropathol* 90: 126-129.
- Krauch, G., E. Wilichowski, et al. (2002). "Pearson marrow-pancreas syndrome with worsening cardiac function caused by pleiotropic rearrangement of mitochondrial DNA." *American Journal of Medical Genetics* 110(1): 57-61.
- Kraytsberg, Y., E. Kudryavtseva, et al. (2006). "Mitochondrial DNA deletions are abundant and cause functional impairment in aged human substantia nigra neurons." *Nat Genet* 38(5): 518-520.
- Larsson, N.-G., H. G. Eiken, et al. (1992). "Lack of Transmission of Deleted mtDNA from a Woman with Kearns-Sayre Syndrome to Her Child." *Am. J. Hum. Genet.* 50: 360-363.
- Lebrecht, D., A. Kokkori, et al. (2005). "Tissue-specific mtDNA lesions and radical-associated mitochondrial dysfunction in human hearts exposed to doxorubicin." *The Journal of Pathology* 207(4): 436-444.
- Lee, H.-C., S.-H. Li, et al. (2004). "Somatic mutations in the D-loop and decrease in the copy number of mitochondrial DNA in human hepatocellular carcinoma." *Mutation Research/Fundamental and Molecular Mechanisms of Mutagenesis* 547(1-2): 71-78.
- Lekrit, P., A. Imsumran, et al. (1999). "A unique 3.5-kb deletion of the mitochondrial genome in Thai patients with Kearns-Sayre syndrome." *Human Genetics* 105(1): 127-131.
- Lezza, A. M. S., A. Cormio, et al. (1997). "Mitochondrial DNA deletions in oculopharyngeal muscular dystrophy." *FEBS Letters* 418(1-2): 167-170.
- Lim, P.-S., Y.-S. Ma, et al. (2002). "Mitochondrial DNA Mutations and Oxidative Damage in Skeletal Muscle of Patients with Chronic Uremia." *Journal of Biomedical Science* 9: 549-560.
- Markaryan, A., E. G. Nelson, et al. (2008). "Detection of mitochondrial DNA deletions in the cochlea and its structural elements from archival human temporal bone tissue." *Mutation Research/Fundamental and Molecular Mechanisms of Mutagenesis* 640(1-2): 38-45.
- Melova, S., J. A. Schneider, et al. (1999). "Mitochondrial DNA rearrangements in aging human brain and in situ PCR of mtDNA." *Neurobiology of Aging* 20(5): 565-571.
- Mita, S., R. Rizzuto, et al. (1990). "Recombination via flanking direct repeats is a major cause of large-scale deletions of human mitochondrial DNA." *Nucleic Acids Research* 18(3): 561-567.
- Mkaouar-Rebai, E., I. Chamkha, et al. (2010). "A case of Kearns-Sayre syndrome with two novel deletions (9.768 and 7.253 kb) of the mtDNA associated with the common deletion in blood leukocytes, buccal mucosa and hair follicles." *Mitochondrion* 10(5): 449-455.
- Moslemi, A.-R., C. Lindberg, et al. (1997). "Analysis of multiple mitochondrial DNA deletions in inclusion body myositis." *Human Mutation* 10(5): 381-386.
- Moslemi, A.-R., A. Melberg, et al. (1996). "Clonal Expansion of Mitochondrial DNA with Multiple Deletions in Autosomal Dominant Progressive External Ophthalmoplegia." *Annals of Neurology* 40(5): 707-713.
- Nakase, H., C. T. Moraes, et al. (1990). "Transcription and Translation of Deleted Mitochondrial Genomes in Kearns-Sayre Syndrome: Implications for Pathogenesis." *Am. J. Hum. Genet.* 46: 418-427.
- Nicholas, A., Y. Kraytsberg, et al. (2009). "On the timing and the extent of clonal expansion of mtDNA deletions: Evidence from single-molecule PCR." *Experimental Neurology* 218(2): 316-319.
- Nicolino, M., T. Ferlin, et al. (1997). "Identification of a Large-Scale Mitochondrial Deoxyribonucleic Acid Deletion in Endocrinopathies and Deafness: Report of Two Unrelated Cases with Diabetes Mellitus and Adrenal Insufficiency, Respectively." *Journal of Clinical Endocrinology & Metabolism* 82(9): 3063-3067.
- Nishigaki, Y., R. Martí, et al. (2004). "ND5 is a hot-spot for multiple atypical mitochondrial DNA deletions in mitochondrial neurogastrointestinal encephalomyopathy." *Human Molecular Genetics* 13(1): 91-101.
- Norby, S., P. Lestienne, et al. (1994). "Juvenile Kearns-Sayre syndrome initially misdiagnosed as a psychosomatic disorder." *Journal of Medical Genetics* 31(1): 45-50.
- Ozawa, T. (1995). "Mechanism of somatic mitochondrial DNA mutations associated with age and diseases." *Biochimica et Biophysica Acta (BBA)* 1271: 177-189.
- Pak, J. W., A. Herbst, et al. (2003). "Mitochondrial DNA mutations as a fundamental mechanism in physiological declines associated with aging." *Aging Cell* 2(1): 1-7.
- Penta, J. S., F. M. Johnson, et al. (2001). "Mitochondrial DNA in human malignancy." *Mutation Research* 488: 119-133.
- Pineda, M., A. Ormazabal, et al. (2006). "Cerebral folate deficiency and leukoencephalopathy caused by a mitochondrial DNA deletion." *Annals of Neurology* 59(2): 394-398.
- Reeve, A. K., K. J. Krishnan, et al. (2008). "Nature of Mitochondrial DNA Deletions in Substantia Nigra Neurons." *The American Journal of Human Genetics* 82(1): 228-235.
- Regan, C. (1999). Sequence Characterization of Breakpoint Regions of Human Mitochondrial DNA Deletions and Possible Mechanisms of Formation. London, Ontario, The University of Western Ontario. Master
- Rocher, C., T. Letellier, et al. (2002). "Base composition at mtDNA boundaries suggests a DNA triple helix model for human mitochondrial DNA large-scale rearrangements." *Molecular Genetics and Metabolism* 76(2): 123-132.
- Rogounovitch, T. I., V. A. Saenko, et al. (2002). "Large Deletions in Mitochondrial DNA in Radiation-associated Human Thyroid Tumors." *Cancer Research* 62(23): 7031-7041.
- Rötig, A., V. Cormier, et al. (1993). "Deletion of mitochondrial DNA in a case of early-onset diabetes mellitus, optic atrophy, and deafness (Wolfram syndrome, MIM 222300)." *The Journal of Clinical Investigation* 91(3): 1095-1098.
- Saiwaki, T., K. Shiga, et al. (2000). "A unique junctional palindromic sequence in mitochondrial DNA from a patient with progressive external ophthalmoplegia." *Molecular Pathology* 53(6): 333-335.
- Samuels, D. C., E. A. Schon, et al. (2004). "Two direct repeats cause most human mtDNA deletions." *Trends in Genetics* 20(9): 393-398.
- Schaefer, A. M., E. L. Blakely, et al. (2005). "Ophthalmoplegia due to mitochondrial DNA disease: The need for genetic diagnosis." *Muscle & Nerve* 32(1): 104-107.
- Schon, E., R. Rizzuto, et al. (1989). "A direct repeat is a hotspot for large-scale deletion of human mitochondrial DNA." *Science* 244(4902): 346-

- Shanske, S., Y. Tang, et al. (2002). "Identical Mitochondrial DNA Deletion in a Woman with Ocular Myopathy and in Her Son with Pearson Syndrome." *The American Journal of Human Genetics* 71(3): 679-683.
- Shoffner, J. M., M. T. Lott, et al. (1989). "Spontaneous Kearns-Sayre/chronic external ophthalmoplegia plus syndrome associated with a mitochondrial DNA deletion: A slip-replication model and metabolic therapy." *Proceedings of the National Academy of Sciences* 86: 7952-7956.
- Solano, A., J. Gámez, et al. (2003). "Characterisation of repeat and palindrome elements in patients harbouring single deletions of mitochondrial DNA." *Journal of Medical Genetics* 40(7): e86.
- Solano, A., G. Russo, et al. (2004). "De Toni-Debré-Fanconi syndrome due to a palindrome-flanked deletion in mitochondrial DNA." *Pediatric Nephrology* 19(7): 790-793.
- Superti-Furga, A., E. Schoenle, et al. (1993). "Pearson bone marrow-pancreas syndrome with insulin-dependent diabetes, progressive renal tubulopathy, organic aciduria and elevated fetal haemoglobin caused by deletion and duplication of mitochondrial DNA." *Eur J Pediatr* 152: 44-50.
- Tang, Y., E. Schon, et al. (2000). "Rearrangements of Human Mitochondrial DNA (mtDNA): New Insights into the Regulation of mtDNA Copy Number and Gene Expression." *Molecular Biology of the Cell* 11: 1471-1485.
- Tengan, C. H., C. Ferreiro-Barros, et al. (2002). "Frequency of duplications in the D-loop in patients with mitochondrial DNA deletions." *Biochimica et Biophysica Acta (BBA) - Molecular Basis of Disease* 1588(1): 65-70.
- Tengan, C. H., B. H. Kiyomoto, et al. (1998). "Mitochondrial Encephalomyopathy and Hypoparathyroidism Associated with a Duplication and a Deletion of Mitochondrial Deoxyribonucleic Acid." *Journal of Clinical Endocrinology & Metabolism* 83(1): 125-129.
- van der Westhuizen, F., J. Smet, et al. (2010). "Aberrant synthesis of ATP synthase resulting from a novel deletion in mitochondrial DNA in an African patient with progressive external ophthalmoplegia." *Journal of Inherited Metabolic Disease*: 1-8.
- Vázquez-Acevedo, M., R. Coria, et al. (1995). "Characterization of a 5025 base pair mitochondrial DNA deletion in Kearns-Sayre syndrome." *Biochimica et Biophysica Acta (BBA)* 1271: 363-368.
- Wanrooij, S., P. Luoma, et al. (2004). "Twinkle and POLG defects enhance age-dependent accumulation of mutations in the control region of mtDNA." *Nucleic Acids Research* 32(10): 3053-3064.
- Yamashita, S., I. Nishino, et al. (2008). "Genotype and phenotype analyses in 136 patients with single large-scale mitochondrial DNA deletions." *J Hum Genet* 53(7): 598-606.
- Zeviani, M. (1992). "Nucleus-Driven Mutations of Human Mitochondrial DNA." *J. Inher. Metab. Dis.* 15: 456-471.
- Zeviani, M., N. Bresolin, et al. (1990). "Nucleus-driven Multiple Large-Scale Deletions of the Human Mitochondrial Genome: A New Autosomal Dominant Disease." *Am. J. Hum. Genet.* 47: 904-914.
- Zeviani, M., S. Servidei, et al. (1989). "An autosomal dominant disorder with multiple deletions of mitochondrial DNA starting at the D-loop region." *Nature* 339(6222): 309-311.
- Zhang, C., A. Baumer, et al. (1992). "Multiple mitochondrial DNA deletions in an elderly human individual." *FEBS Letters* 297(1-2): 34-38.

**Supplemental Figure S2. Refinement of breakpoint locations on the revised Cambridge reference mtDNA sequence (rCRS).** In cases where one or more bases could be equally aligned upstream or downstream of the deletion area, we corrected the limits of the deletion by retaining all of the possible matches at the 5' breakpoint.

rCRS ACACCAACCACCAA (...) TTACTATCCATCCTCA

ACACCAA - - - - - (...) - - - - - CATCCTCA - after Muscle alignment

ACACCAAC  (...) - - - - - ATCCTCA - after correction

**Supplemental Figure S3. List of the 753 unique mtDNA deletions used in this study.** Numbers according to the L-strand positions of the revised Cambridge reference mtDNA sequence (rCRS; NC\_012920).

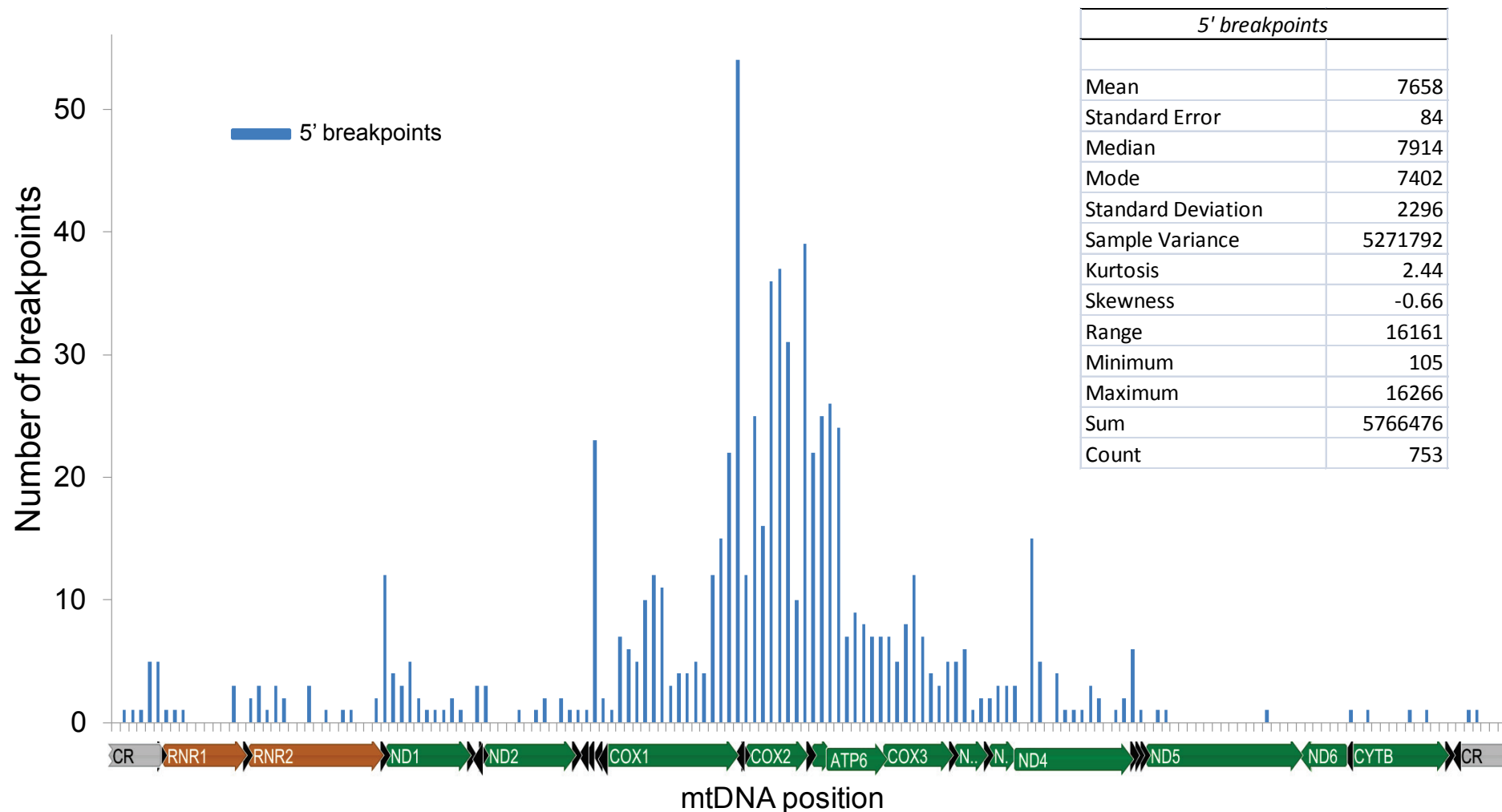
Breakpoints		3393	16072	5803	16072	6625	16074
5'	3'	3418	3432	5836	12662	6634	9925
105	112	3432	16071	5987	13537	6750	16072
299	349	3486	16068	6003	15441	6753	16075
306	357	3549	15440	6019	6025	6759	15865
463	12080	3549	16072	6023	14424	6790	15918
471	5152	3571	15540	6062	16070	6836	14380
478	5160	3575	15968	6074	9179	6843	14388
488	8643	3591	11519	6076	13799	6851	14816
493	14242	3614	12987	6084	13808	6862	13061
504	5443	3692	16068	6124	15893	6919	13564
537	4431	3742	16074	6128	15434	6927	16072
544	13768	3826	16071	6172	13057	6935	15447
547	4443	3963	11432	6173	16078	6940	15451
585	4443	4048	15949	6175	14162	6961	16071
633	16262	4069	14306	6189	16072	7057	16071
708	13767	4141	16073	6203	14258	7067	16047
898	16116	4351	16071	6215	10976	7098	16072
1417	15219	4376	16078	6218	13447	7099	16071
1491	5206	4398	14822	6226	13447	7113	14693
1491	5323	4458	16074	6238	14103	7115	10546
1672	16071	4469	13923	6310	15611	7116	16073
1691	13925	4486	16075	6320	11272	7122	14000
1741	14502	4882	16068	6326	13989	7125	13050
1753	13101	5042	14552	6326	13990	7127	14393
1771	16072	5173	15607	6326	16071	7128	14006
1840	5451	5195	16071	6329	13994	7182	14566
1906	16072	5328	16076	6331	13994	7185	14120
1907	16079	5330	16077	6341	13994	7188	14335
1989	14366	5440	13030	6341	14005	7193	14587
2059	16071	5561	13405	6380	14096	7193	14596
2068	16074	5671	16071	6416	14182	7201	14809
2333	16075	5745	16073	6422	15208	7204	13903
2333	16078	5772	13411	6423	14344	7212	14261
2334	16073	5773	13411	6428	15270	7215	16072
2540	16047	5781	16069	6429	14101	7215	16073
2781	16071	5781	16071	6437	14077	7218	16071
2818	16078	5782	13483	6453	14288	7235	16072
3167	14154	5785	13923	6464	14874	7235	16074
3173	14161	5785	16072	6466	14135	7265	16035
3212	16071	5787	13920	6469	15586	7265	16071
3233	3237	5787	13924	6476	13777	7267	16077
3255	16070	5787	15576	6476	14146	7268	16077
3256	16072	5787	16035	6504	13805	7277	12300
3263	15123	5787	16071	6521	16071	7288	15900
3263	16070	5787	16072	6527	15055	7289	14943
3263	16071	5787	16073	6533	16075	7322	13464
3263	16072	5788	13239	6537	13838	7322	15239
3263	16073	5788	15448	6551	13852	7323	15056
3270	16034	5788	16069	6555	14345	7323	15435
3272	15068	5788	16071	6572	12304	7329	14531
3272	16034	5789	16075	6577	15154	7331	15946
3311	15741	5793	12767	6585	15144	7337	14931
3326	3591	5795	13920	6587	14285	7338	14598
3326	13923	5798	16072	6601	16284	7347	14245

7350	16071	7479	11440	7804	13795	7978	16072
7360	15276	7485	10997	7805	13844	7982	15504
7366	14060	7491	11004	7808	12388	7983	15504
7367	12063	7493	13985	7811	16071	7989	15435
7367	16072	7494	12763	7813	16077	7990	16068
7370	16072	7494	16073	7814	14805	7990	16078
7370	16073	7495	15439	7815	13581	7991	16070
7372	13239	7506	14433	7817	14536	7991	16073
7374	15957	7508	15939	7817	15382	7992	15730
7387	15930	7517	13096	7817	16071	7992	16072
7396	13118	7524	13395	7817	16072	7995	15213
7399	15383	7527	16065	7817	16074	7997	15568
7399	15405	7529	13474	7818	16075	7998	12300
7400	14290	7539	15237	7818	16077	8019	15519
7401	16068	7539	15913	7819	16070	8030	16070
7401	16074	7547	13475	7819	16077	8030	16075
7402	13677	7553	13546	7820	16074	8030	16078
7402	15128	7562	15381	7821	13760	8031	14564
7402	15372	7563	13724	7821	16072	8031	16070
7402	16068	7623	15036	7821	16073	8031	16074
7402	16071	7626	8196	7823	15389	8031	16077
7402	16072	7629	14813	7824	16077	8032	12300
7402	16073	7629	16072	7828	13385	8032	16069
7402	16076	7632	8206	7829	14135	8032	16071
7403	12392	7635	15310	7841	13905	8032	16072
7403	16075	7635	15440	7845	15761	8032	16073
7403	16078	7638	15916	7846	9749	8032	16075
7404	16080	7644	16071	7850	13474	8033	14337
7406	14560	7662	15429	7853	13887	8033	16071
7407	12396	7662	15552	7857	12283	8033	16078
7407	13620	7667	14359	7869	16069	8034	11423
7409	13688	7667	16071	7869	16076	8034	11434
7410	13688	7667	16072	7870	16076	8034	15882
7414	14568	7669	13810	7885	15698	8034	16071
7414	15609	7669	15437	7889	15435	8034	16076
7428	13415	7669	16072	7899	15642	8036	13095
7429	14895	7671	16071	7904	16285	8049	14115
7431	15093	7677	15013	7912	9560	8053	15444
7439	13477	7682	13722	7914	16070	8055	13095
7440	15882	7694	14053	7915	16276	8058	12215
7443	13468	7695	13107	7919	16072	8076	15911
7448	13451	7696	12365	7920	16078	8083	16071
7448	13475	7696	13987	7921	16072	8093	16071
7449	15167	7697	12364	7921	16080	8095	12393
7449	15926	7705	15945	7921	16283	8113	14849
7450	15378	7719	16053	7922	16075	8134	13573
7452	12263	7723	14108	7923	11423	8137	14771
7452	13723	7723	14110	7923	16075	8143	15271
7453	13487	7728	13806	7931	15761	8151	15783
7453	13644	7733	16073	7933	15604	8156	16037
7453	15435	7755	15236	7945	16073	8170	16333
7460	11847	7756	16072	7945	16074	8175	16073
7461	12977	7775	13532	7949	14315	8176	11614
7462	16071	7775	16072	7958	15927	8198	13433
7465	11426	7777	13794	7959	13787	8208	16070
7469	14285	7779	16071	7961	13374	8211	15340
7470	16074	7792	14181	7962	16020	8213	16070
7471	16073	7794	12561	7964	12432	8220	13998
7472	14814	7795	15287	7967	11312	8222	13476
7477	15998	7795	16073	7975	15496	8231	16072

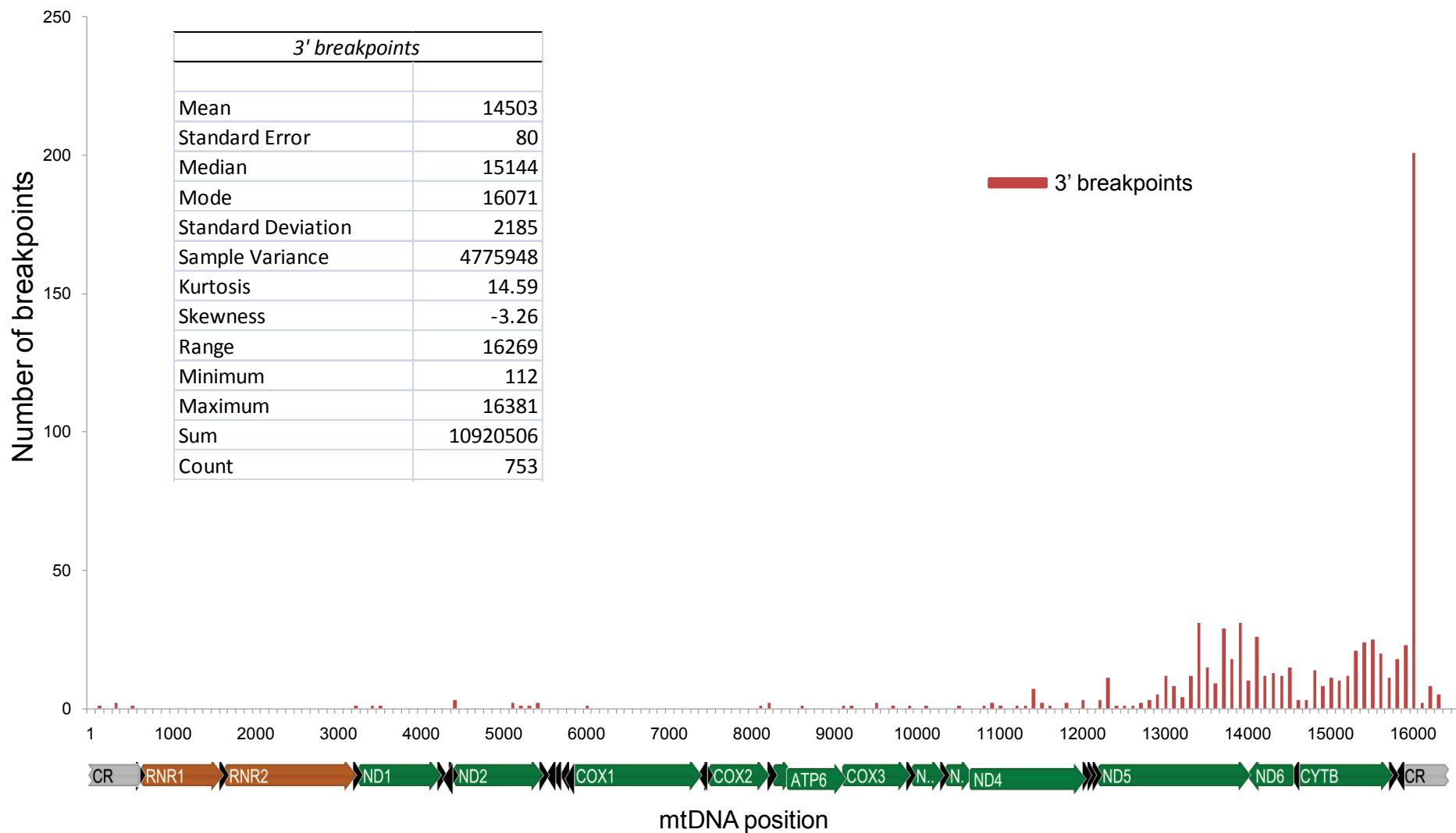
8231	16280	8421	12399	8637	16236	9417	13684
8232	15542	8421	13564	8640	13378	9436	15913
8232	16071	8426	12894	8640	15369	9440	14083
8233	13383	8428	15482	8645	15656	9444	13964
8233	13967	8437	14068	8648	16085	9484	13724
8233	16067	8439	16075	8651	16071	9486	9502
8239	13407	8441	14505	8662	14817	9490	16072
8240	13341	8461	15603	8663	16075	9497	13735
8244	16381	8464	13138	8664	15363	9514	13052
8250	13410	8467	13444	8697	15938	9515	13055
8253	16066	8468	13446	8707	13723	9532	14135
8254	16070	8470	13447	8711	13550	9537	15519
8256	15261	8475	14381	8712	15990	9538	15537
8257	16162	8476	14812	8723	9215	9538	15658
8259	13359	8477	13590	8728	13699	9574	10166
8261	15652	8479	13594	8775	13991	9574	12972
8262	10844	8482	13460	8777	14006	9574	13951
8263	13531	8483	13448	8810	15638	9576	13942
8264	16071	8484	13448	8813	13304	9587	13953
8268	14906	8491	13448	8815	15846	9591	13052
8269	13447	8503	13425	8817	15610	9603	14141
8271	13410	8518	15422	8823	15855	9609	14147
8278	13770	8527	13718	8825	15658	9622	15812
8280	8290	8536	15439	8830	14897	9625	15435
8281	16371	8536	15642	8838	14906	9659	11536
8287	16072	8547	15727	8893	15503	9665	15183
8289	13791	8553	15585	8904	14903	9698	13735
8291	16276	8555	13980	8905	14110	9729	15338
8292	16034	8561	13985	8933	13768	9744	14439
8294	16074	8562	13759	8989	13997	9773	13756
8295	16073	8563	14596	8992	16072	9799	15557
8299	13153	8563	15435	8992	16074	9816	15744
8299	16071	8564	16072	8993	13563	9845	16065
8304	15055	8569	15879	8996	16070	9860	15026
8305	14619	8571	13237	9009	16354	9923	16073
8308	13382	8572	13997	9016	14576	9924	15194
8310	16078	8572	15826	9021	13833	9966	15801
8312	13667	8576	12984	9070	13476	9995	15897
8316	15802	8576	13962	9079	15312	9998	15895
8327	13358	8576	16075	9084	15438	10004	15360
8344	15633	8577	15731	9087	13155	10051	15077
8372	12085	8580	15239	9137	13808	10063	14598
8373	16067	8580	15539	9143	13333	10071	14622
8380	13338	8583	15958	9144	13816	10080	14959
8385	15918	8587	15738	9180	14281	10104	11868
8387	12821	8588	13730	9191	12909	10154	15945
8387	15515	8601	15731	9191	15322	10169	14435
8387	16067	8612	13575	9194	15323	10186	13759
8387	16071	8612	16072	9238	15576	10191	13753
8387	16078	8617	13877	9246	13058	10198	13761
8394	16070	8623	15662	9253	14425	10207	13766
8395	16071	8623	15663	9258	13627	10367	12829
8395	16073	8624	13886	9258	14429	10370	15570
8398	16072	8624	15662	9268	16068	10418	15570
8398	16073	8630	16067	9281	13810	10497	14760
8408	14118	8631	13513	9320	14273	10559	14981
8412	15664	8631	13580	9345	13148	10587	15913
8417	15127	8635	16074	9345	13851	10598	13206
8418	14127	8637	16073	9351	13154	10625	13059
8420	11498	8637	16084	9357	13865	10668	14859

10676	14868	10953	14133	11368	15786	12113	14421
10746	14125	10953	15837	11479	16071	12113	14422
10749	14129	10961	15846	11514	13810	12122	15844
10758	14138	10969	14119	11648	13811	12203	15355
10925	14152	10984	15543	11668	15916	12439	15390
10935	13773	11035	15159	11680	14258	12544	15525
10939	15530	11035	15183	11731	14450	13761	14252
10940	15546	11036	15028	11739	15572	14786	14791
10943	15363	11036	15441	11986	13792	14927	14943
10943	15372	11065	15860	12021	16075	15497	15522
10946	13781	11232	13980	12084	15854	15643	15665
10951	15372	11237	13984	12103	14414	16164	16319
10952	13990	11240	15036	12104	14413	16266	576
10952	15373	11258	14369	12112	14422		

**Supplemental Figure S4. Distribution of 5' deletion breakpoints in the human mtDNA.** The values were grouped in 100-nt windows. The locations of the mitochondrial genes are shown below the x-axis.



**Supplemental Figure S5. Distribution of 3' deletion breakpoints in the human mtDNA.** The values were grouped in 100-nt windows. The locations of the mitochondrial genes are shown below the x-axis.



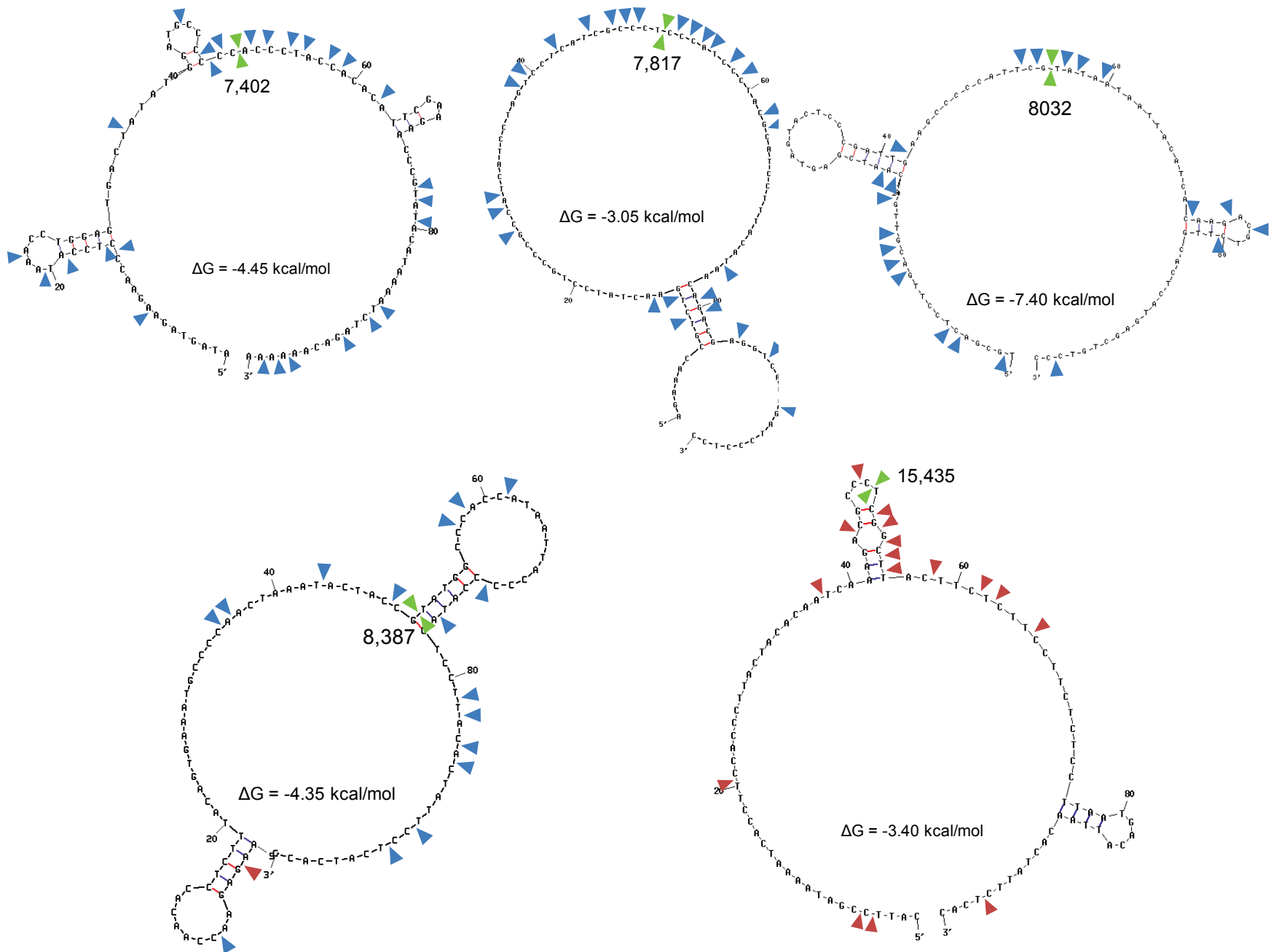
**Supplemental Figure S6. Distribution of 3' breakpoints around the 16,071 hotspot.**

mtDNA position	Number of 3' breakpoints	
	n	%
<b>16065</b>	2	0.27
<b>16066</b>	1	0.13
<b>16067</b>	4	0.53
<b>16068</b>	7	0.93
<b>16069</b>	4	0.53
<b>16070</b>	13	1.73
<b>16071</b>	41	5.44
<b>16072</b>	38	5.05
<b>16073</b>	23	3.05
<b>16074</b>	14	1.86
<b>16075</b>	15	1.99
<b>16076</b>	5	0.66
<b>16077</b>	8	1.06
<b>16078</b>	11	1.46
<b>16079</b>	1	0.13
<b>16080</b>	2	0.27
<b>Total</b>	<b>189</b>	<b>25.09</b>

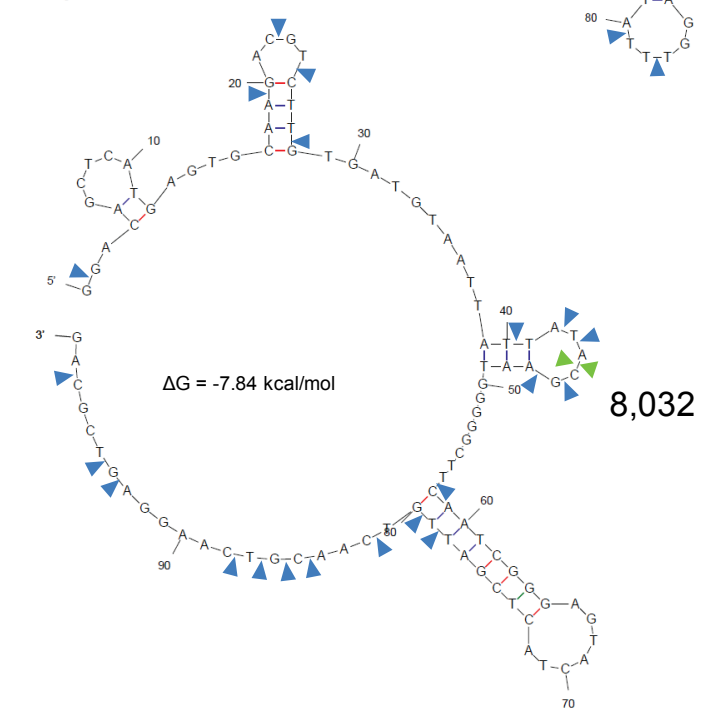
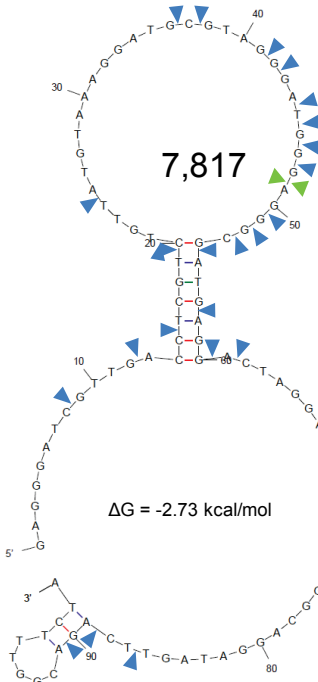
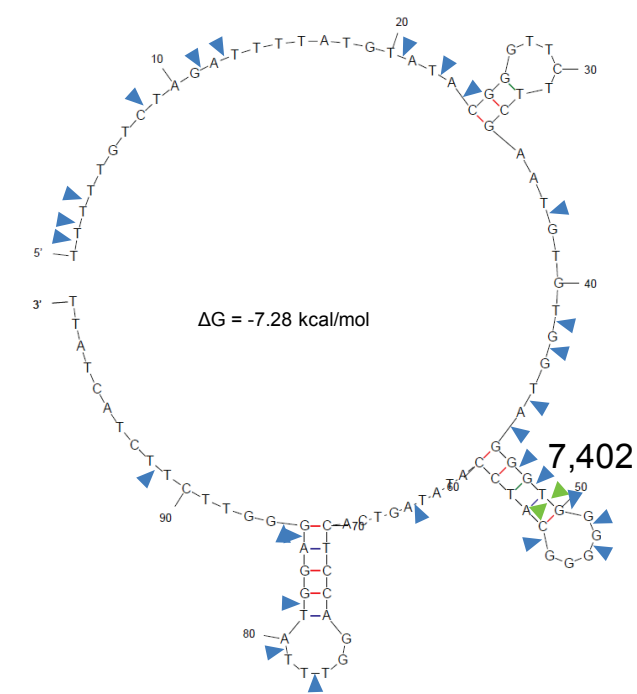
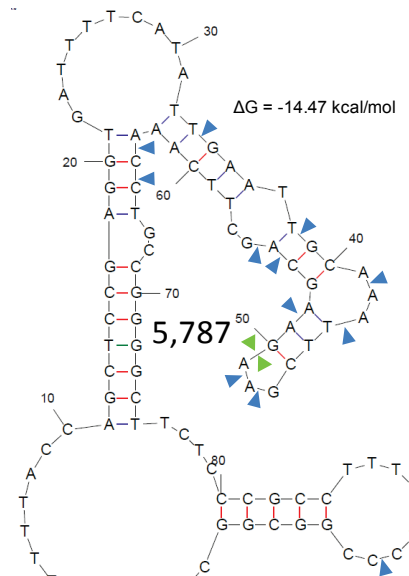
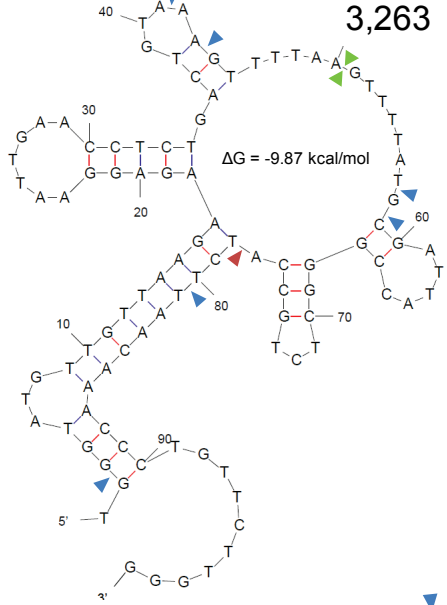
**Supplemental Figure S7. List of the most frequent breakpoints detected in real and simulated mtDNA deletions.** In cases where adjacent sites had several breakpoints, only the most frequent one in that cluster is represented. The dataset of 20,000 random deletions was generated using in-house python scripts.

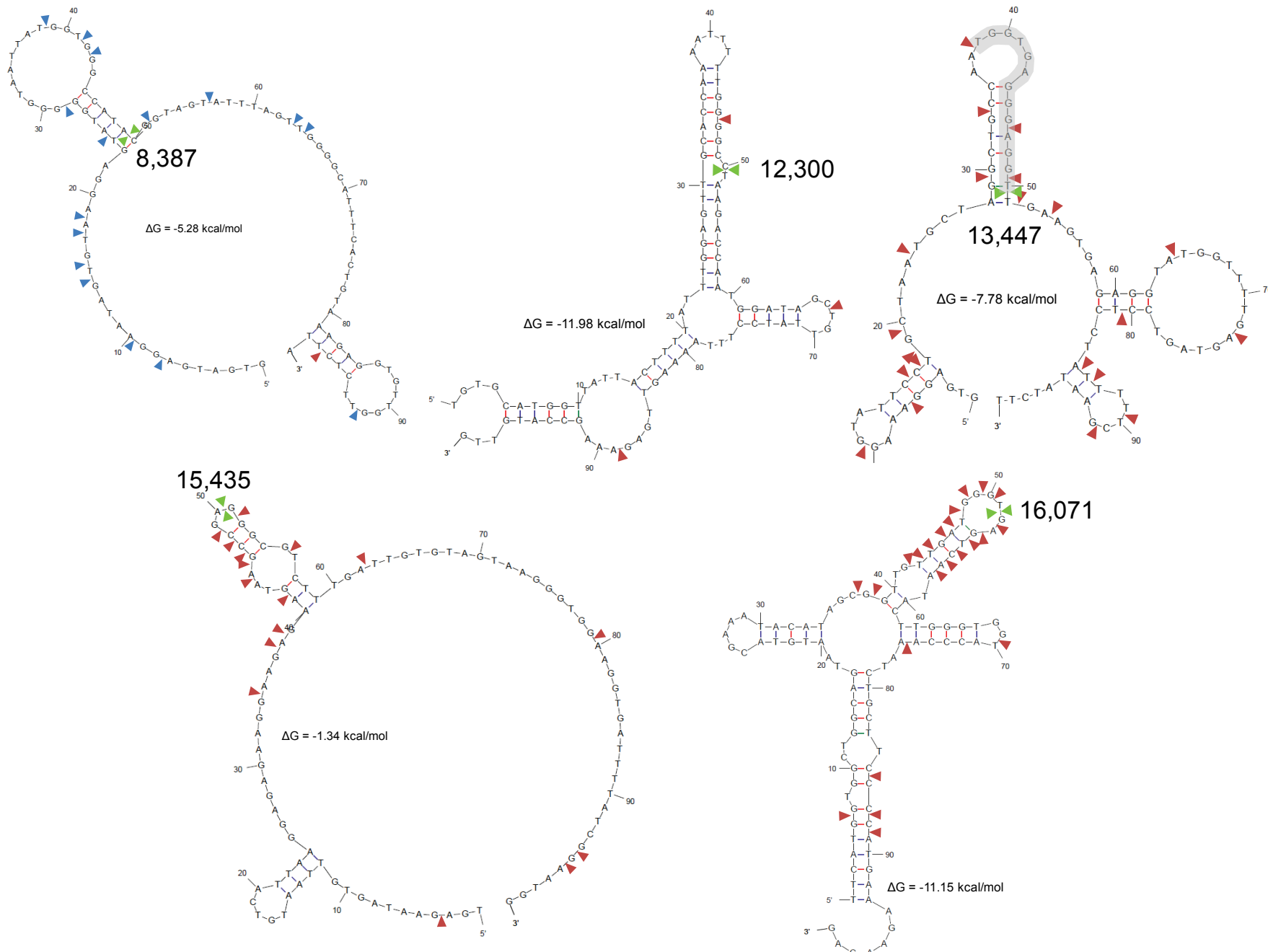
mtDNA position	Type	n	Frequency
<b>753 real deletions</b>			
16,071	3'	41	5.4X10 <sup>-2</sup>
7,402	5'	8	1.1X10 <sup>-2</sup>
5,787	5'	7	9.3X10 <sup>-3</sup>
15,435	3'	6	8.0X10 <sup>-3</sup>
8,032	5'	6	8.0X10 <sup>-3</sup>
3,263	5'	5	6.6X10 <sup>-3</sup>
7,817	5'	5	6.6X10 <sup>-3</sup>
8,387	5'	5	6.6X10 <sup>-3</sup>
13,447	3'	4	5.3X10 <sup>-3</sup>
12,300	3'	3	4.0X10 <sup>-3</sup>
<b>20,000 random deletions</b>			
13,556	5'	8	4.0X10 <sup>-4</sup>
14,291	5'	8	4.0X10 <sup>-4</sup>
4,613	3'	7	3.5X10 <sup>-4</sup>
9,529	3'	7	3.5X10 <sup>-4</sup>
13,312	3'	7	3.5X10 <sup>-4</sup>
4,255	5'	7	3.5X10 <sup>-4</sup>
4,443	5'	7	3.5X10 <sup>-4</sup>
6,785	5'	7	3.5X10 <sup>-4</sup>
8,198	5'	7	3.5X10 <sup>-4</sup>
9,682	5'	7	3.5X10 <sup>-4</sup>
16,156	5'	7	3.5X10 <sup>-4</sup>

**Supplemental Figure S8. Secondary structures around the most frequent 5' and 3' breakpoint sites of the human mtDNA L-strand.** The 100-nt windows around five of the ten most frequent breakpoint sites (mtDNA positions 7,402, 7,817, 8,032, 8,387, 15,435, indicated by green arrows) were used for folding predictions with the UNAFold software package. The breakpoints were used as window midpoints. The blue and red arrows indicate less frequent 5' and 3' breakpoints, respectively. The secondary structures were obtained in the mfold-util software v4.6.

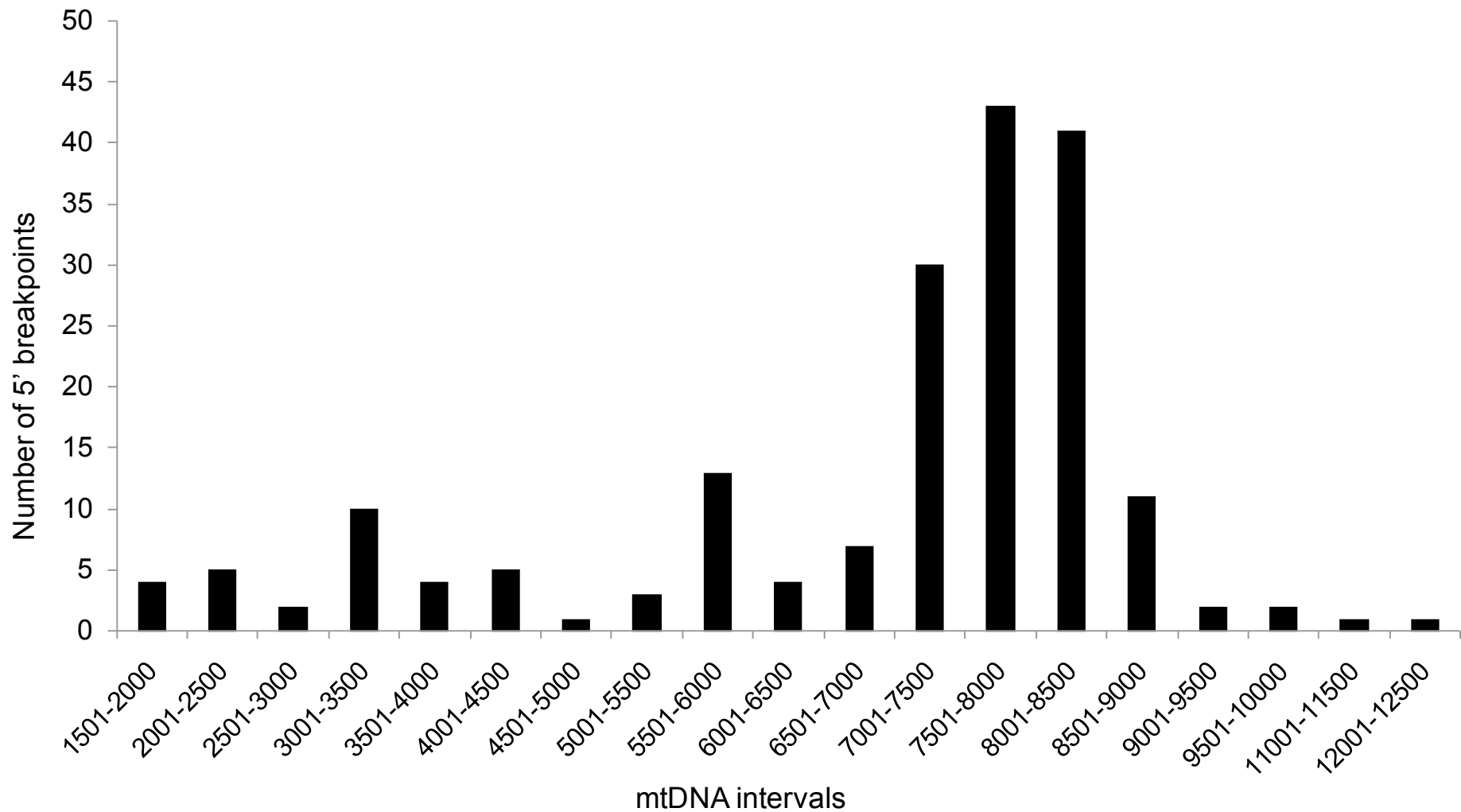


**Supplemental Figure S9. Secondary structures around the most frequent 5' and 3' breakpoint sites of the human mtDNA H-strand.** The 100-nt windows around the ten most frequent breakpoint sites (mtDNA positions 3,263, 5,787, 7,402, 7,817, 8,032, 8,387, 12,300, 13,447, 15,435 and 16,071 indicated by green arrows) were used for folding predictions with the UNAFold software package. The breakpoints were used as window midpoints. The blue and red arrows indicate less frequent 5' and 3' breakpoints, respectively. Highlighted in grey is the 13-bp direct repeat at the 3' breakpoint of the 'common deletion'. The secondary structures were obtained in the mfold-util software v4.6.

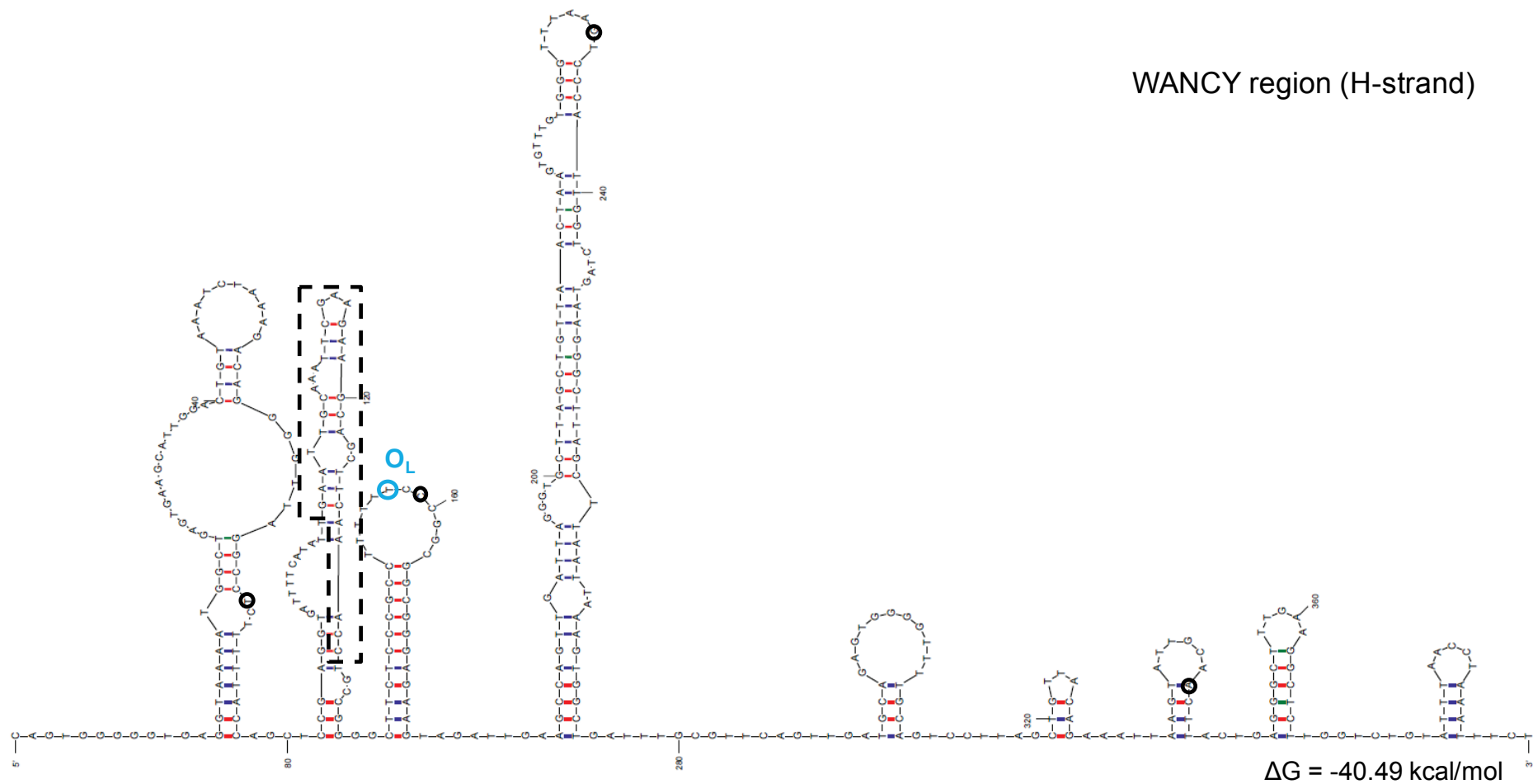




**Supplemental Figure S10. Global distribution of 5' breakpoints from deletions with the 3' breakpoint at the 16,071 hotspot.** The graph displays the distribution of 5' breakpoints (binned in 500-nt intervals along the mtDNA sequence) from deletions with a 3' breakpoint in the 16,075-16,080 mtDNA region.



**Supplemental Figure S11. The WANCY cluster of tRNAs is a hotspot for mtDNA breakage.** The 27 5' deletion breakpoints (black circles and dashed line) identified in the WANCY region are located in hairpin elements predicted for the H-strand. The blue circle depicts the origin of L-strand replication ( $O_L$ ). The secondary structure was obtained in the mfold-util software v4.6.



**Supplemental Figure S12. Distribution of deletion breakpoints according to the coding features of the mitochondrial genome.**

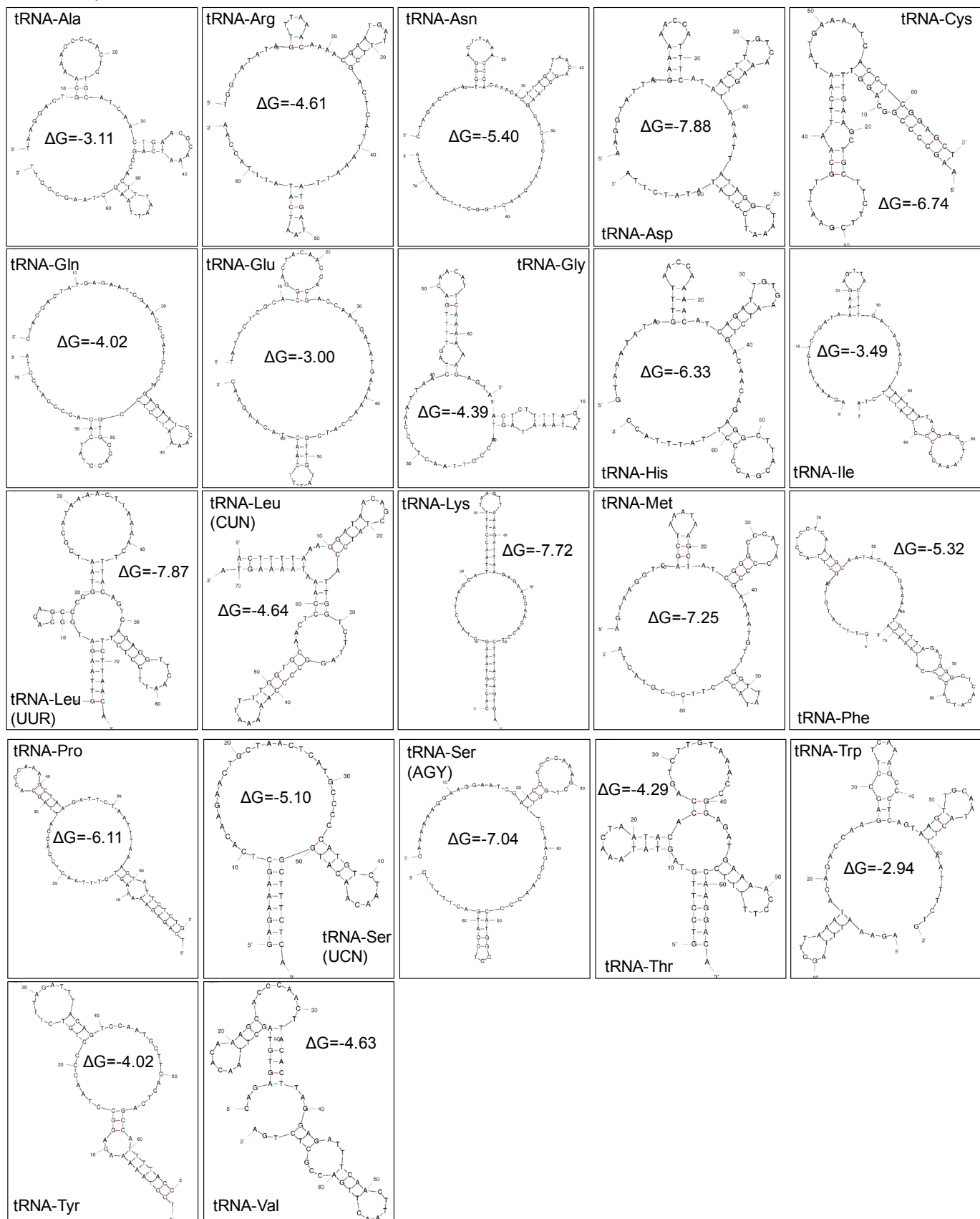
mtDNA region	mtDNA position (first - last)		Length (bases)	Number of breakpoints			% of total breakpoints
				5'	3'	Total	
<i>tRNA-Phe</i>	577	647	71	2	0	2	0.13
<i>RNR1</i>	648	1601	954	5	0	5	0.33
<i>tRNA-Val</i>	1602	1670	69	0	0	0	0.00
<i>RNR2</i>	1671	3229	1559	20	0	20	1.33
<i>tRNA-Leu(UUA/G)</i>	3230	3304	75	11	1	12	0.80
<i>ND1</i>	3307	4262	956	20	2	22	1.46
<i>tRNA-Ile</i>	4263	4331	69	0	0	0	0.00
<i>tRNA-Gln</i>	4329	4400	72	3	0	3	0.20
<i>tRNA-Met</i>	4402	4469	68	2	3	5	0.33
<i>ND2</i>	4470	5511	1042	8	6	14	0.93
<i>tRNA-Trp</i>	5512	5579	68	1	0	1	0.07
<i>tRNA-Ala</i>	5587	5655	69	0	0	0	0.00
<i>tRNA-Asn</i>	5657	5729	73	1	0	1	0.07
<i>tRNA-Cys</i>	5761	5826	66	23	0	23	1.53
<i>tRNA-Tyr</i>	5826	5891	66	1	0	1	0.07
<i>COX1</i>	5904	7445	1542	149	1	150	9.96
<i>tRNA-Ser(UCN)</i>	7446	7514	69	28	0	28	1.86
<i>tRNA-Asp</i>	7518	7585	68	9	0	9	0.60
<i>COX2</i>	7586	8269	684	182	2	184	12.22
<i>tRNA-Lys</i>	8295	8364	70	11	0	11	0.73
<i>ATP8</i>	8366	8572	207	56	0	56	3.72
<i>ATP6</i>	8527	9207	681	71	2	73	4.85
<i>COX3</i>	9207	9990	784	49	5	54	3.59
<i>tRNA-Gly</i>	9991	10058	68	4	0	4	0.27
<i>ND3</i>	10059	10404	346	12	1	13	0.86
<i>tRNA-Arg</i>	10405	10469	65	1	0	1	0.07
<i>ND4L</i>	10470	10766	297	10	1	11	0.73
<i>ND4</i>	10760	12137	1378	41	21	62	4.12
<i>tRNA-His</i>	12138	12206	69	1	0	1	0.07
<i>tRNA-Ser(AGY)</i>	12207	12265	59	0	2	2	0.13
<i>tRNA-Leu(CUN)</i>	12266	12336	71	0	5	5	0.33
<i>ND5</i>	12337	14148	1812	3	219	222	14.74
<i>ND6</i>	14149	14673	525	0	60	60	3.98
<i>tRNA-Glu</i>	14674	14742	69	0	1	1	0.07
<i>CYTB</i>	14747	15887	1141	4	174	178	11.82
<i>tRNA-Thr</i>	15888	15953	66	0	21	21	1.39
<i>tRNA-Pro</i>	15956	16023	68	0	0	0	0.00
<b>Control region (CR)</b>	16024	576	1122	14	219	233	15.47
<b>Non-coding (other than CR)</b>		89	11	7	18		1.20

Breakpoints located in overlapping genes were only considered once

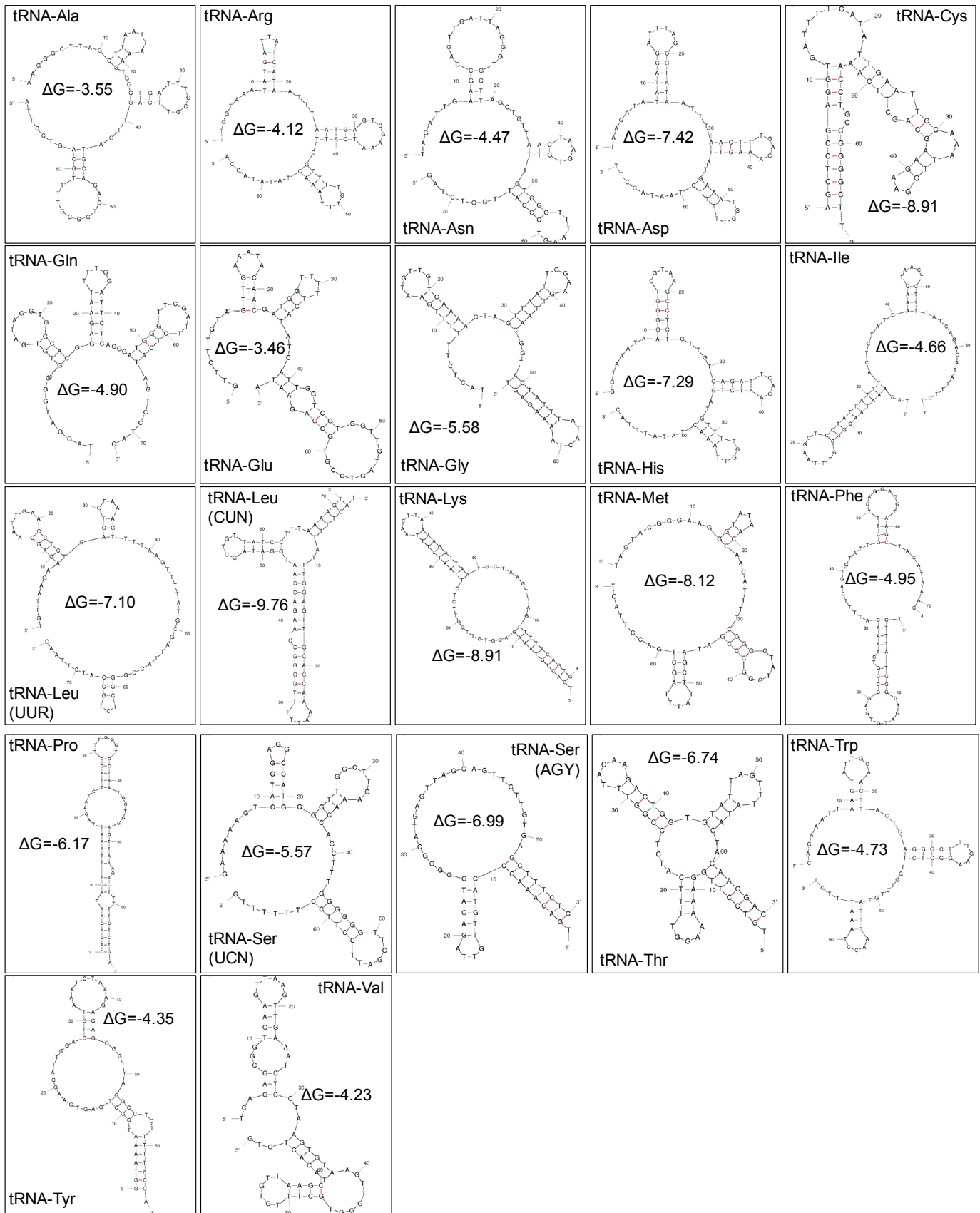
**Supplemental Figure S13. Number of mtDNA deletion breakpoints per base.** The breakpoints were grouped according to the coding features of the mitochondrial genome.

mtDNA region	Breakpoints/base		
	5'	3'	Total
<i>tRNA-Phe</i>	0.028	0.000	0.028
<i>RNR1</i>	0.005	0.000	0.005
<i>tRNA-Val</i>	0.000	0.000	0.000
<i>RNR2</i>	0.013	0.000	0.013
<i>tRNA-Leu(UUA/G)</i>	0.147	0.013	0.160
<i>ND1</i>	0.021	0.002	0.023
<i>tRNA-Ile</i>	0.000	0.000	0.000
<i>tRNA-Gln</i>	0.042	0.000	0.042
<i>tRNA-Met</i>	0.029	0.044	0.074
<i>ND2</i>	0.008	0.006	0.013
<i>tRNA-Trp</i>	0.015	0.000	0.015
<i>tRNA-Ala</i>	0.000	0.000	0.000
<i>tRNA-Asn</i>	0.014	0.000	0.014
<i>tRNA-Cys</i>	0.348	0.000	0.348
<i>tRNA-Tyr</i>	0.015	0.000	0.015
<i>COX1</i>	0.097	0.001	0.097
<i>tRNA-Ser(UCN)</i>	0.406	0.000	0.406
<i>tRNA-Asp</i>	0.132	0.000	0.132
<i>COX2</i>	0.266	0.003	0.269
<i>tRNA-Lys</i>	0.157	0.000	0.157
<i>ATP8</i>	0.271	0.000	0.271
<i>ATP6</i>	0.104	0.003	0.107
<i>COX3</i>	0.063	0.006	0.069
<i>tRNA-Gly</i>	0.059	0.000	0.059
<i>ND3</i>	0.035	0.003	0.038
<i>tRNA-Arg</i>	0.015	0.000	0.015
<i>ND4L</i>	0.034	0.003	0.037
<i>ND4</i>	0.030	0.015	0.045
<i>tRNA-His</i>	0.014	0.000	0.014
<i>tRNA-Ser(AGY)</i>	0.000	0.034	0.034
<i>tRNA-Leu(CUN)</i>	0.000	0.070	0.070
<i>ND5</i>	0.002	0.121	0.123
<i>ND6</i>	0.000	0.114	0.114
<i>tRNA-Glu</i>	0.000	0.014	0.014
<i>CYTB</i>	0.004	0.152	0.156
<i>tRNA-Thr</i>	0.000	0.318	0.318
<i>tRNA-Pro</i>	0.000	0.000	0.000
<b>Control region (CR)</b>	0.012	0.195	0.208
<b>Non-coding (other than CR)</b>	0.124	0.079	0.202

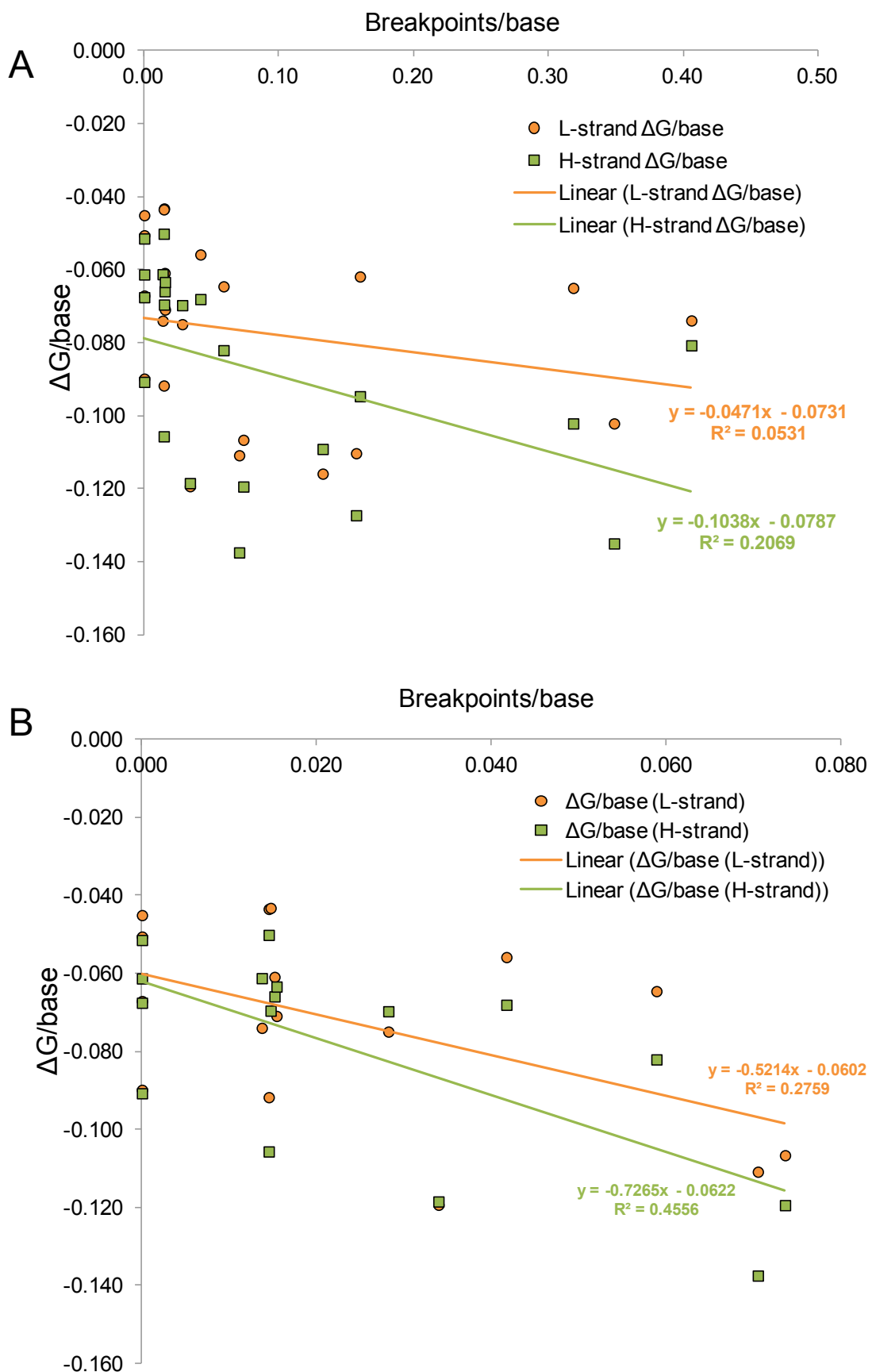
**Supplemental Figure S14. Secondary structures of mitochondrial tRNA genes (L-strand).** The secondary structures were obtained in the mfold-util software v4.6.  $\Delta G$  values in kcal/mol.



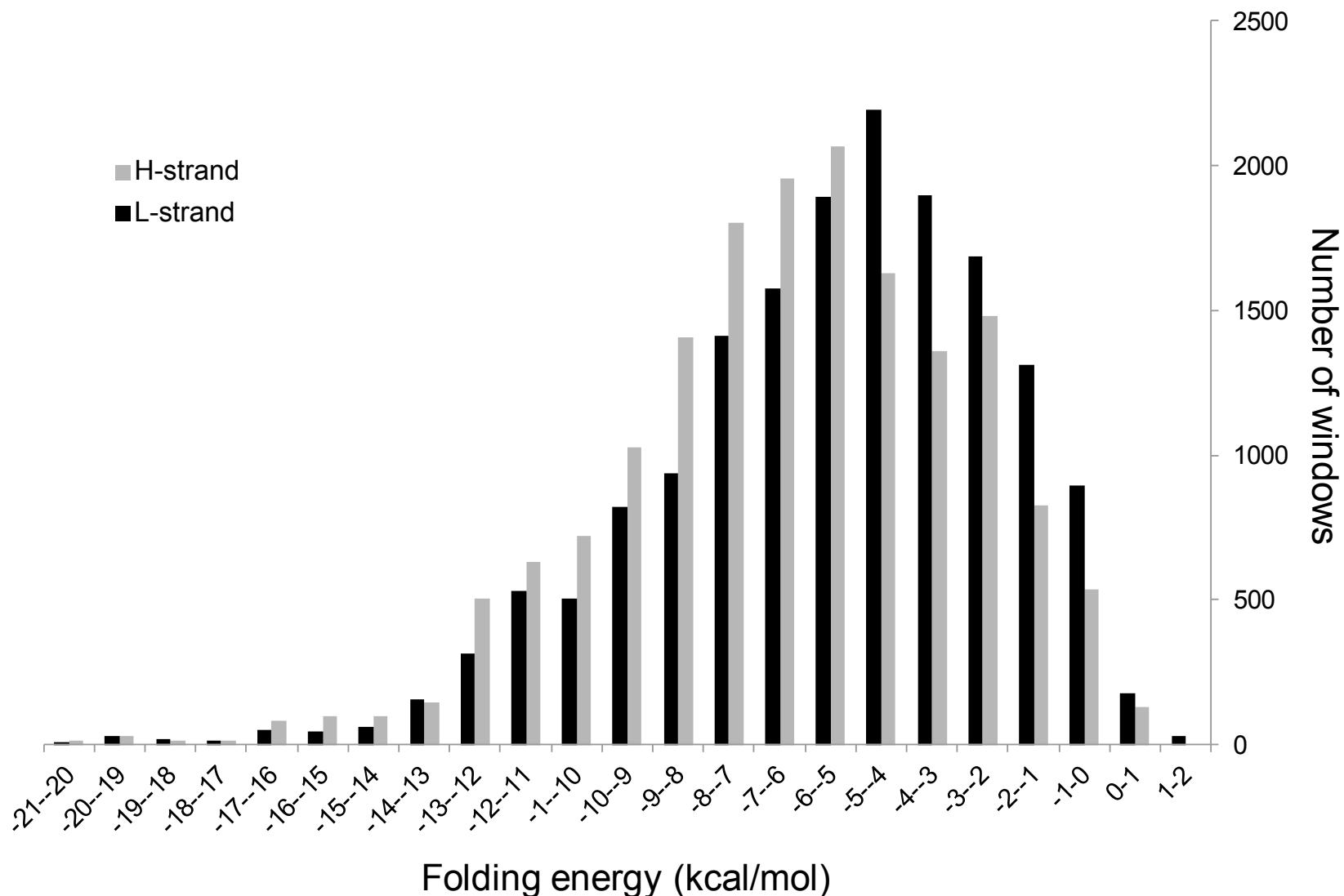
**Supplemental Figure S15. Secondary structures of mitochondrial tRNA genes (H-strand).** The secondary structures were obtained in the mfold-util software v4.6.  $\Delta G$  values in kcal/mol.



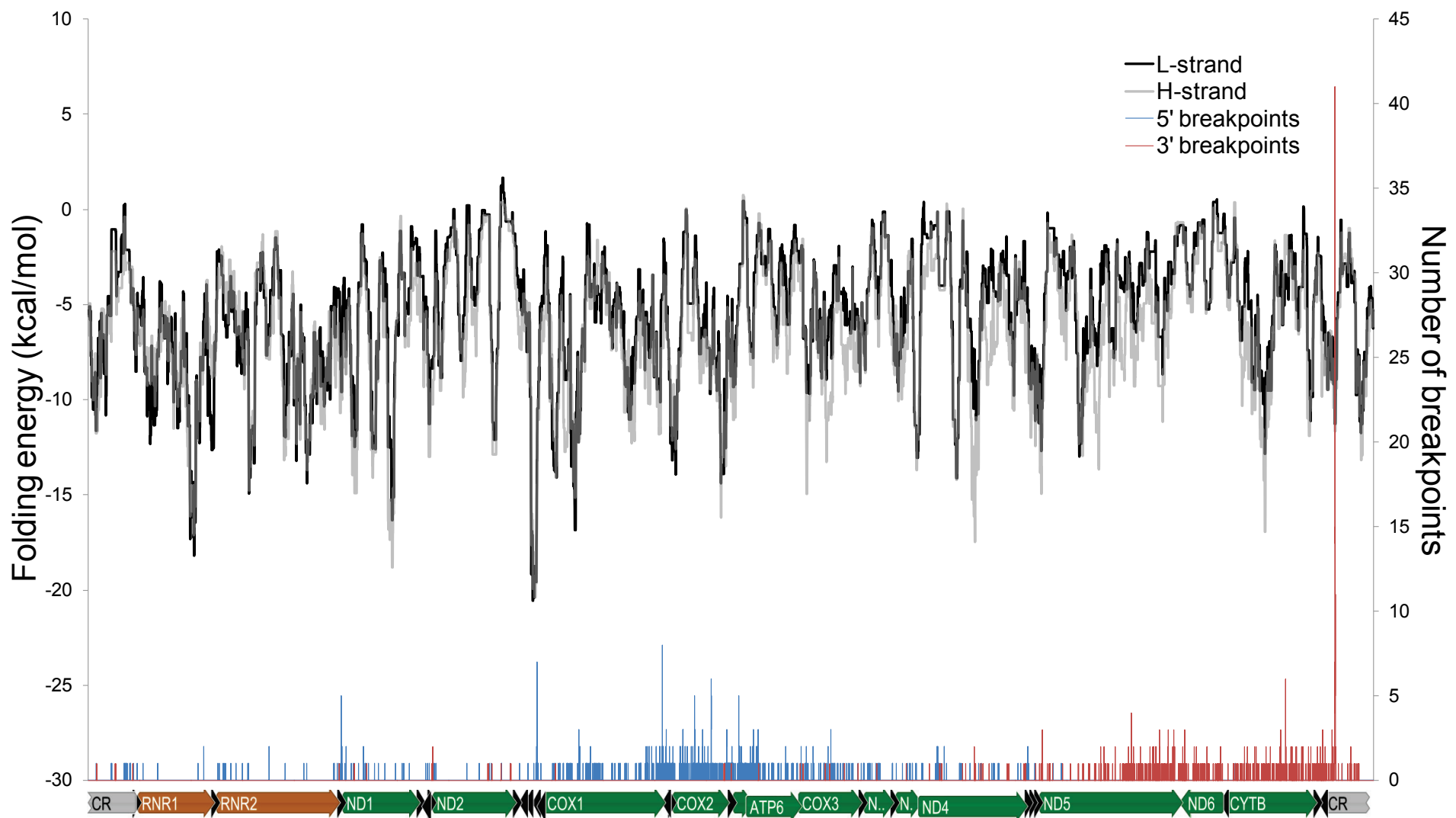
**Supplemental Figure S16. Relationship between the folding free energy and the number of breakpoints in tRNA genes.** (A) All tRNA gene sequences. (B) Only tRNA genes with less than 0.1 breakpoints per base. The linear trendlines are indicated for L- and H-strand tRNA gene sequences.



**Supplemental Figure S17. The distribution of folding energies predicted for all of the 100-nt windows of the mitochondrial genome.** The distribution of folding energies in 16,569 windows (length of 100 nt, overlapped by 1 nt) is shown for the L-strand (black bars) and H-strand (grey bars).



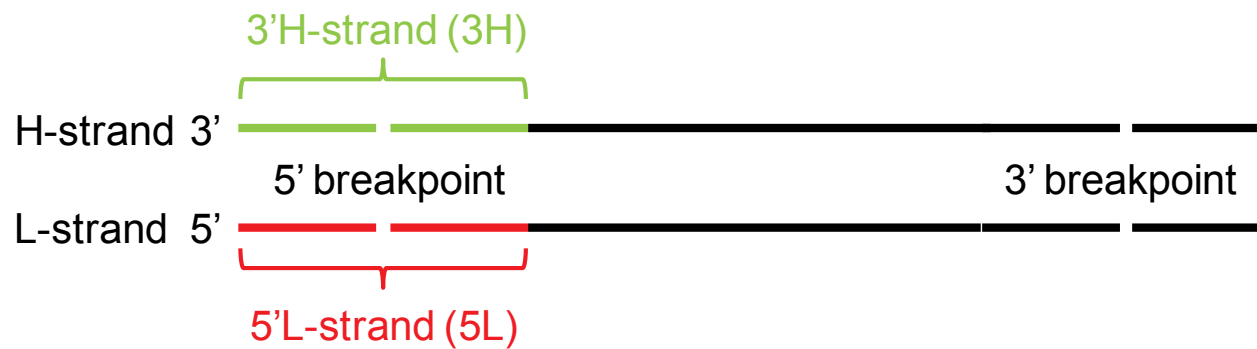
**Supplemental Figure S18. Deletion hotspots and the mtDNA regions with high folding potentials.** The profile of folding energy across the mitochondrial genome (sliding window of 100-nt with 1-nt overlap) is shown for the L-strand (black line) and H-strand (grey line). The distribution of 5' (blue bars) and 3' (red bars) deletion breakpoints is also indicated. The locations of the mitochondrial genes are shown below the x-axis.



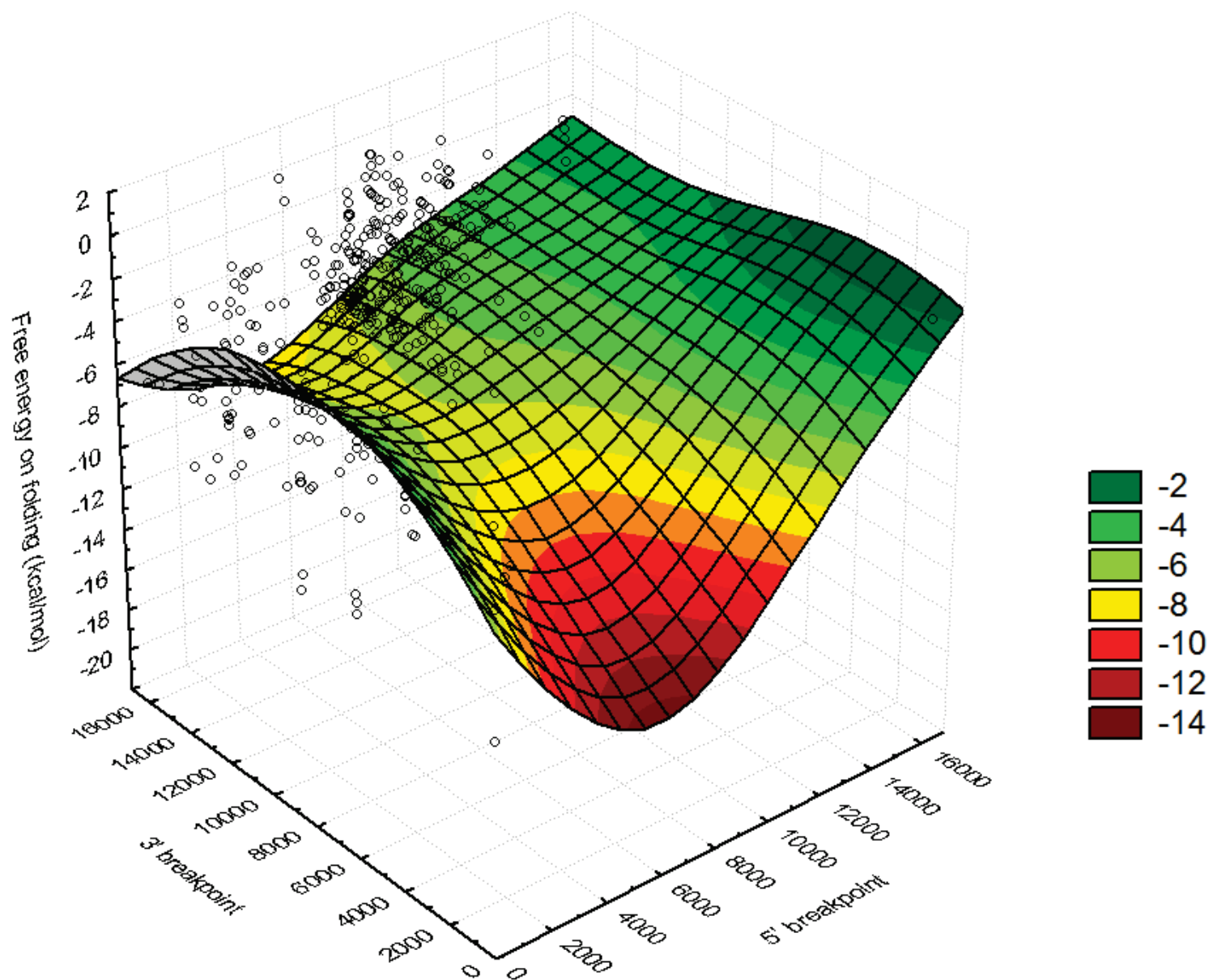
**Supplemental Figure S19. Descriptive statistics of folding energies in deletion breakpoints areas.** The energy of folding (kcal/mol) was estimated for the four 100-nt areas (in both H- and L-strands) around 5' and 3' breakpoints (breakpoints as midpoints) from 753 reported mtDNA deletions.

<b>Breakpoint area</b>	<b>Mean</b>	<b>Median</b>	<b>Mode</b>	<b>Minimum</b>	<b>Maximum</b>	<b>Range</b>
<b>5L</b>	-5.66	-5.38	-4.450	-19.580	1.27	20.85
<b>3L</b>	-5.93	-5.04	-11.27	-13.900	1.23	15.13
<b>3H</b>	-6.58	-6.73	-7.280	-19.900	0.76	20.66
<b>5H</b>	-7.01	-6.87	-11.65	-17.460	0.38	17.84

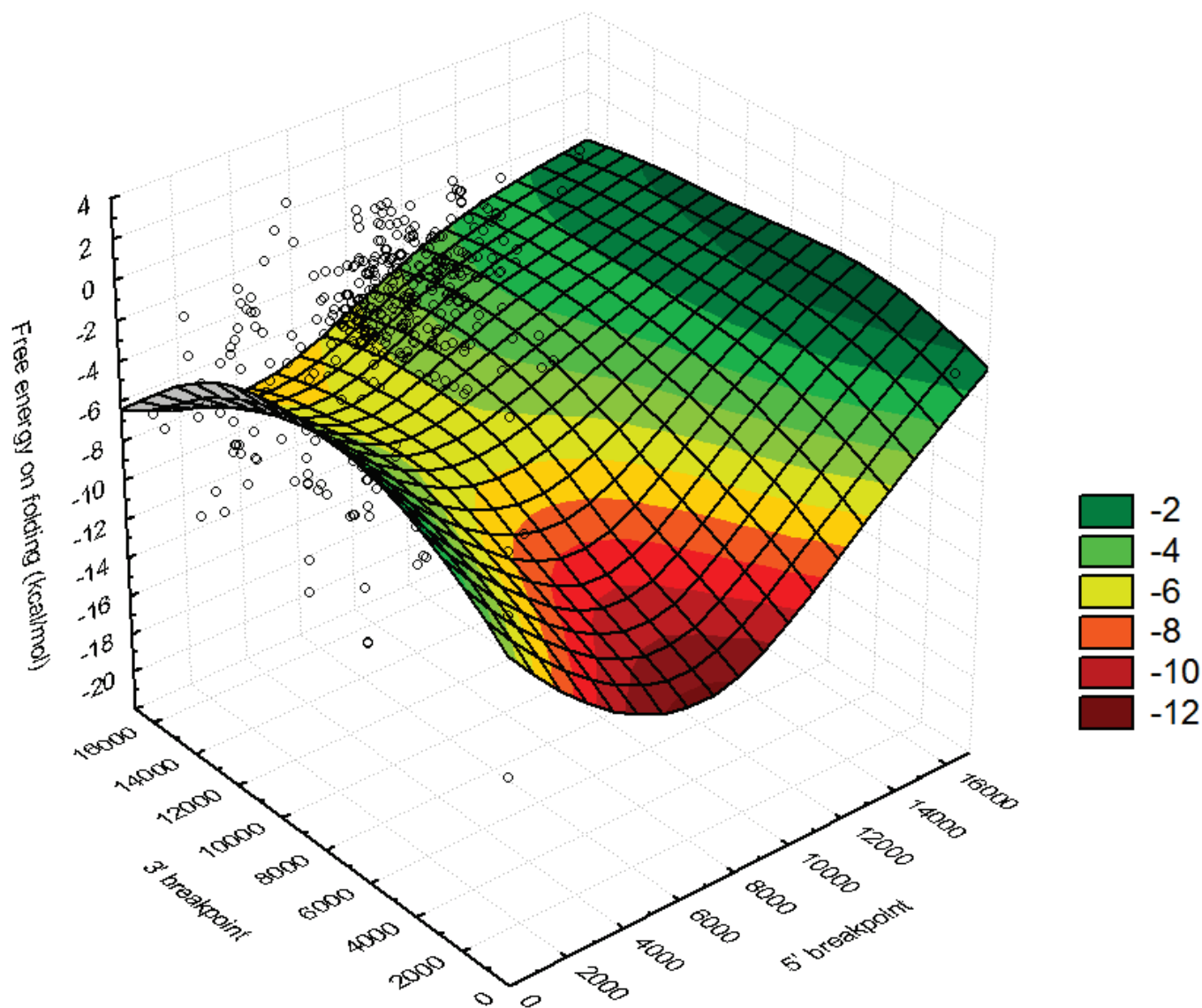
**Supplemental Figure S20. Landscape of the folding potentials in the 5' breakpoint areas of mtDNA deletions.** The three-dimensional plots display the locations of breakpoints (X and Y axes) according to the free energy of folding of the breakpoint area (z-axis). A surface is fitted to the data according to the distance-weighted least-squares smoothing procedure. A gradient from red (high folding potential) to green (low folding potential) is used in both graphs.



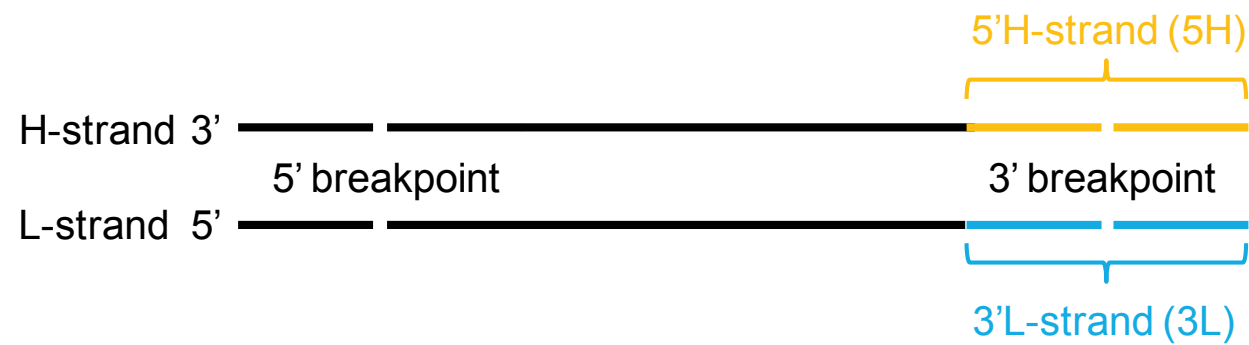
3H



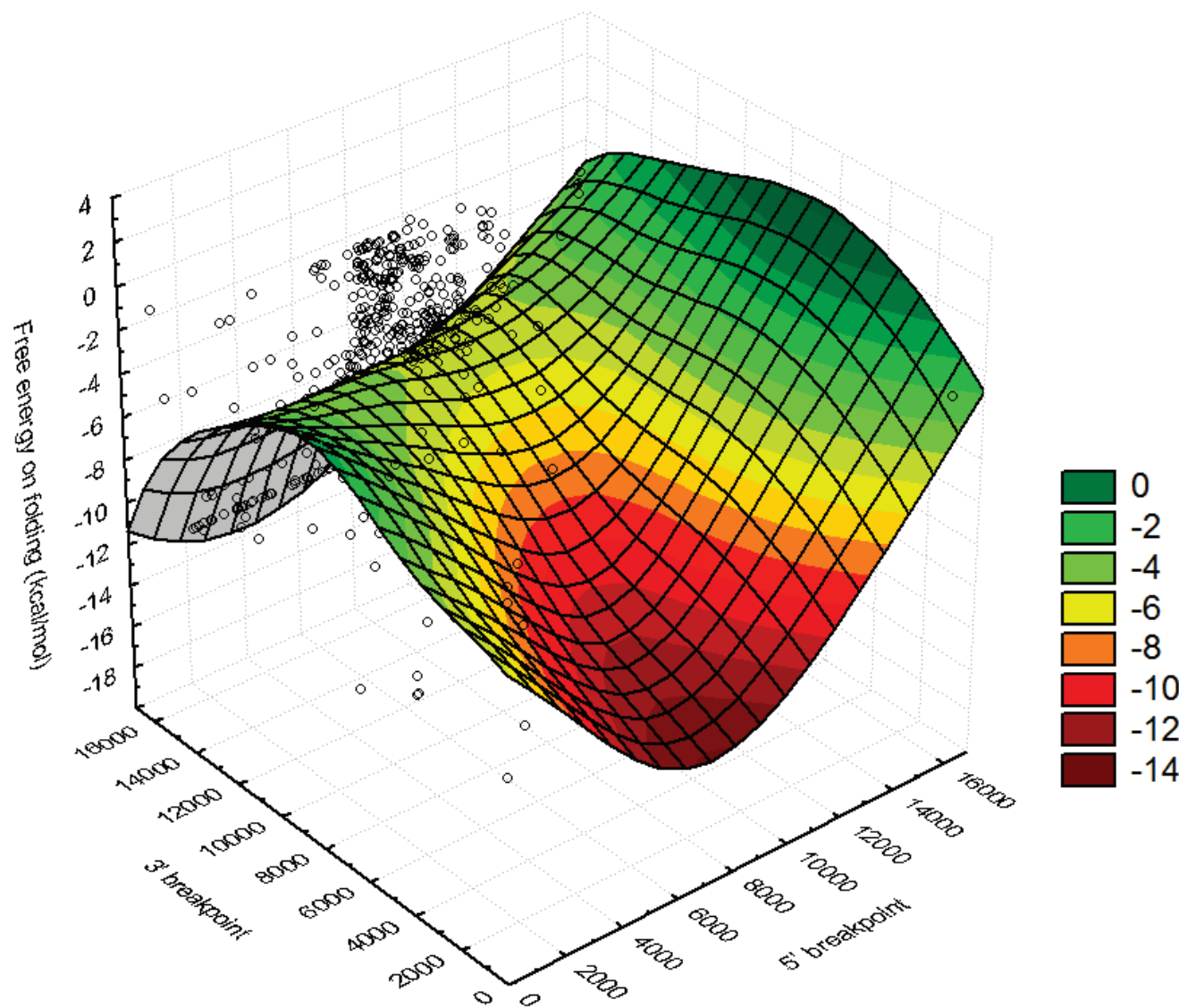
5L



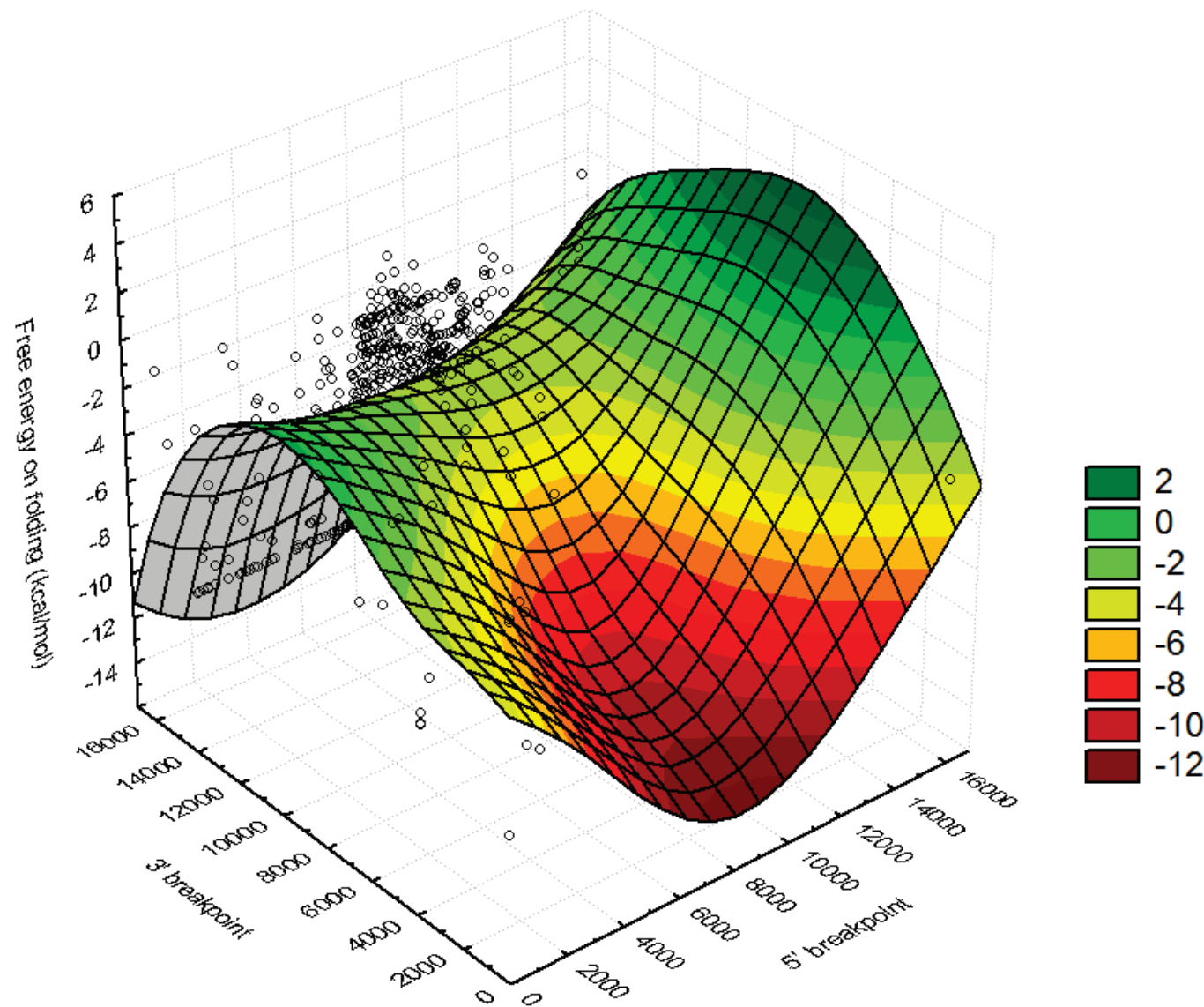
**Supplemental Figure S21. Landscape of the folding potentials in the 3' breakpoint area of mtDNA deletions.** The three-dimensional plots display the locations of breakpoints (X and Y axes) according to the free energy of folding of the breakpoint area (z-axis). A surface is fitted to the data according to the distance-weighted least-squares smoothing procedure. A gradient from red (high folding potential) to green (low folding potential) is used in both graphs.



5H



3L



**Supplemental Figure S22. Comparison between the two main breakpoint hotspots and their flanking regions.** The table displays the genomic location, number of breakpoints and mean ΔG values for the two mtDNA segments where 5' and 3' breakpoints are more frequent and their upstream and downstream flanking segments with the same length.

	Upstream region	Breakpoint hotspot	Downstream region	Upstream region	Breakpoint hotspot	Downstream region
<b>mtDNA region (length)</b>	6,601 - 7,400 (800 nt)	7,401 - 8,200 (800 nt)	8,201 - 9,000 (800 nt)	6,601 - 7,400 (800 nt)	7,401 - 8,200 (800 nt)	8,201 - 9,000 (800 nt)
<b>Gene or noncoding feature</b>	<i>COX1</i> (partial)	<i>COX1</i> (partial) / <i>tRNA-Ser</i> / <i>tRNA-Asp</i> / <i>COX2</i> (partial)	<i>COX2</i> (partial) / <i>tRNA-Lys</i> / <i>ATP8</i> / <i>ATP6</i> (partial)	<i>COX1</i> (partial)	<i>COX1</i> (partial) / <i>tRNA-Ser</i> / <i>tRNA-Asp</i> / <i>COX2</i> (partial)	<i>COX2</i> (partial) / <i>tRNA-Lys</i> / <i>ATP8</i> / <i>ATP6</i> (partial)
<b>Parameter</b>	Number of 5' breakpoints (per base)			Mean ΔG (kcal/mol)		
<b>Value</b>	70 (0.09)	220 (0.28)	160 (0.20)	-6.18	-6.76	-4.26
<b>p-value</b>		9.29x10 <sup>-12</sup>	1.36x10 <sup>-2</sup>		4.21x10 <sup>-5</sup>	< 1.00x10 <sup>-17</sup>
<b>mtDNA region (length)</b>	15,901 – 16,000 (100 nt)	16,001 - 16,100 (100 nt)	16,101-16,200 (100 nt)	15,901 – 16,000 (100 nt)	16,001 - 16,100 (100 nt)	16,101-16,200 (100 nt)
<b>Gene or noncoding feature</b>	<i>tRNA-Thr</i> (partial) / <i>tRNA-Pro</i> (partial)	<i>tRNA-Pro</i> (partial) / control region (partial)	control region (partial)	<i>tRNA-Thr</i> (partial) / <i>tRNA-Pro</i> (partial)	<i>tRNA-Pro</i> (partial) / control region (partial)	control region (partial)
<b>Parameter</b>	Number of 3' breakpoints (per base)			Mean ΔG (kcal/mol)		
<b>Value</b>	22 (0.22)	201 (2.01)	2 (0.02)	-6.97	-8.32	-3.40
<b>p-value</b>		7.05x10 <sup>-3</sup>	2.78x10 <sup>-3</sup>		1.85x10 <sup>-11</sup>	< 1.00x10 <sup>-17</sup>